Snow Conditions in the Pacific Northwest: Near Real-Time Monitoring and Future Projections

Hordur Bragi Helgason

A thesis
submitted in partial fulfillment of the
requirements for the degree of

Master of Science in Civil Engineering

University of Washington
2016

Committee:
Bart Nijssen
Jessica Lundquist

Program Authorized to Offer Degree:
Civil and Environmental Engineering

University of Washington

Abstract

Snow conditions in the Pacific Northwest: Near Real-Time Monitoring and Future Projections

Hordur Bragi Helgason

Chair of Supervisory Committee:
Professor Bart Nijssen
Civil and Environmental Engineering

In the Pacific Northwest (PNW), a large part of the annual precipitation falls as snow in the mountains during fall and winter. The winter snowpack is an important reservoir of water in the region, naturally storing water for the dry period during spring and summer. Water resource managers in the region need to keep track of how much snow resides in the mountains and how much moisture is contained in soils. They also need to have an idea of what the future holds in terms of snow accumulation for long-term planning. We describe a near real-time monitoring system of hydrological variables we have implemented over the PNW as part of the Northwest Climate Toolbox, an ongoing project by collaborators in the Pacific Northwest Climate Impacts Research Consortium (CIRC). Furthermore, we examine projected changes in snow conditions in the PNW during the 21st century. For this purpose, we take advantage of a large number of hydrological simulations made as part of a new study to evaluate climate change impacts on the hydrology of the Columbia River Basin. With projected average increases in winter temperature in the range of 2.6°C to 4.8°C by the end of the century, widespread declines in snow accumulations are projected. These declines in snow accumulations are expected to be greatest in the Cascades, especially the southern portion and western slopes, and in the Olympics. Higher elevated areas with historic mean winter temperatures of less than -6 °C show more resistance to climate warming. The choice of climate model seems to be the major source of uncertainty in model results. By comparing the recent snow drought year of 2015 to our projections, we are able to contextualize the future snow conditions in an intuitive way for resource managers. To offer a practical application, we also examine the implications of less snow for ski resorts in the region.

Acknowledgements

I would like to thank my advisor, Professor Bart Nijssen, for his mentorship and guidance throughout this project. I would also like to thank the Valle Scholarship and Scandinavian Exchange Program for giving me the opportunity to study towards my graduate degree here at the University of Washington. This project is also supported in part by the Bonneville Power Administration, Bureau of Reclamation, and the National Oceanic and Atmospheric Administration. This work would not have been possible without the assistance and previous work completed by Marisa Baptiste and Oriana Chegwidden, and the help from Yixin Mao, Elizabeth Clark, Joseph Hamman and Diana Gergel.

Table of contents

1. Introduction

The North American Pacific Northwest (PNW) is a region that experiences wide varieties of climates. Most of the annual precipitation in the area occurs during the winter months, of which the largest share falls in the mountains as snow. The hydrology of rivers in the area is thus dominated by the cycle of snow accumulation and melt. The attributes of water supply systems in the PNW vary across the area with its highly diverse hydroclimatology.

In this thesis, we focus our efforts on two different facets of the hydrology of the PNW. In chapter 2, we describe a near real-time monitoring system of hydrologic variables (soil moisture and snow conditions) that we have implemented over the PNW as part of a larger project called the Northwest Climate Toolbox. In chapter 3, we examine projected changes in snow conditions in the PNW during the 21st century, using a large number of hydrological simulations made as a part of an ongoing study to evaluate climate change impacts on the hydrology of the Columbia River Basin.

2. Near real-time monitoring of hydrologic variables as part of the NW Climate Toolbox

2.1 Introduction

The attributes of water supply systems in the Pacific Northwest of the United States (PNW) vary across the area with its highly diverse hydroclimatology. For example, water in the humid areas west of the Cascades is primarily managed for municipal water supply and hydropower production (Shukla et al., 2011). In the arid and semiarid areas east of the Cascades, water is primarily managed for agricultural water supply and, in the case of the Columbia River system, hydropower production (Shukla et al., 2011). All areas in the PNW have in common that monitoring hydrological conditions is essential for a variety of purposes, especially given that droughts can cause significant economic losses (e.g. Xiao et al., 2016). In the Pacific Northwest (PNW), a large part of the annual precipitation falls as snow in the mountains during fall and winter. The winter snowpack is an important reservoir of water in the region, naturally storing water for the dry period during spring and summer. Being able to monitor snow conditions is therefore important for water resource managers in the region.

The Northwest Climate Toolbox is an ongoing project by collaborators in the Pacific Northwest Climate Impacts Research Consortium (CIRC). The goal of the project is to provide stakeholders and policy makers in the PNW with accessible climate information and easy-to-use decision support tools on the web. An important part of the project is to integrate surface water monitoring into the Toolbox. Since 2005, the University of Washington has operated a surface water monitor for the United States (Wood and Lettenmaier 2006; Wood 2008; Shukla et al., 2011). The monitor provides near real-time information on soil moisture (SM), snow water equivalent (SWE) and total moisture (TM; sum of SM and SWE) over the region. We have integrated the same hydrologic monitoring capability into the Northwest Climate Toolbox, but have streamlined and simplified the computing infrastructure compared to the previous system. The Variable Infiltration Capacity (VIC; Liang et al., 1994) model is run at a 1/16th degree scale across the PNW on a daily basis. The Toolbox provides means to interpret current conditions at a point or over a region by comparing them to a historic reference period.

In this chapter of the thesis, I explain the technical and operational aspects of the hydrologic components of the NW Climate Toolbox, what tools we have used to build it and how we intend to move forward.

2.2 Approach

2.2.1 Domain

The domain currently being monitored is the U.S. part of the Columbia River basin and the region's coastal drainages (Figure 2.1). The domain covers parts of 7 US states, mainly Washington, Oregon, Idaho and Montana (and portions of Wyoming, Utah and Nevada). The total number of 1/16th degree grid cells within this domain is 20,790. The domain is bounded by the Rocky Mountains to the east and north, the Pacific Ocean to the west and the Great Basin to the south.

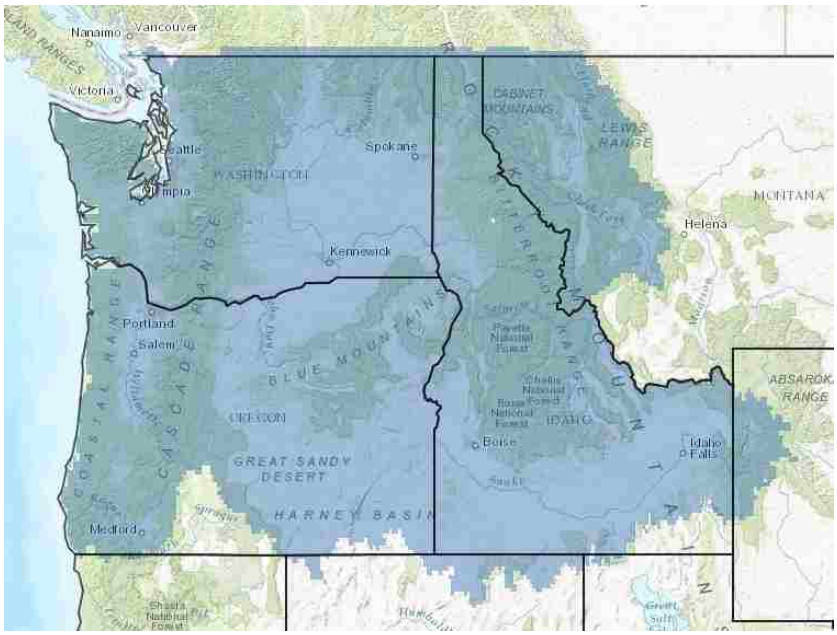

Figure 2.1: The domain currently being monitored in the NW Climate Toolbox is shown in blue (the Columbia River Basin and coastal drainages). The total number of 1/16th degree grid cells is 20,790.

This area has a highly diverse range in elevations and experiences wide varieties of climates. Areas west of the Cascades generally have a maritime climate, characterized by cool, dry summers and mild, wet winters. The climate on the eastern side of the Cascades is continental, characterized by warm, dry summers and cold, clear winters (Sumioka et al., 1998). An alpine climate dominates in the Rocky Mountains.

The Columbia River originates at Columbia Lake in British Columbia's Rocky Mountains. It flows from Canada into the United States and eventually reaches the Pacific Ocean

near Astoria, Oregon. On average, about 25 percent of the Columbia River flow comes from the part of the basin that lies in Canada's province of British Columbia (BPA 2001). The northern Rockies are highly elevated and most of the winter precipitation there falls as snow. Even though the importance of monitoring soil moisture and especially SWE in this area is high, this part of the basin is not currently a part of our monitoring domain. The meteorological forcings we use to force our hydrologic model (see sections 2.2.2 and 2.2.3) are currently only provided for the United States. Our collaborators are in the process of expanding the meteorological dataset to include Canada. We will thus soon be able to expand our monitoring domain to include the entire Columbia River basin.

2.2.2 Hydrologic modeling

The hydrologic model used for this project is the Variable Infiltration Capacity (VIC) hydrologic model (Liang et al., 1994). VIC is a semi-distributed hydrologic model that solves the energy and water balance equations at every grid cell, typically at resolutions ranging from a fraction of a degree to several degrees latitude and longitude. In our implementation, VIC version 5.0.1 (Hamman et al., 2016) is run in energy balance mode at a 3-hour time step at a spatial resolution of 1/16th degrees. As inputs, we use maximum and minimum temperature, wind, specific humidity, shortwave radiation and precipitation in addition to fixed topography and land cover characteristics. Figure 2.2 shows the basic structure of the model.

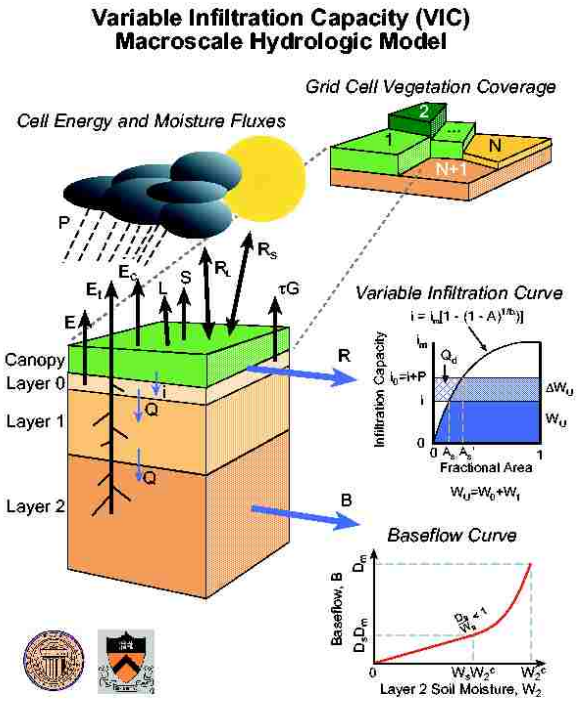

Figure 2.2: Schematic of the VIC model showing its basic structure (Figure source: Gao et al., 2010.

The VIC model assumes a statistical representation of the sub-scale spatial variability in topography, soil and vegetation. Therefore, the model allows infiltration capacities, runoff generation and evapotranspiration to vary within each grid cell. The sub-grid scale spatial variability in topography is especially important when simulating the accumulation and ablation of snow in complex terrain. Using the topography information the model divides the grid cell into elevation bands. The dry adiabatic lapse rate is used to lapse the grid-cell average temperature to each elevation band, and precipitation falls as snow or rain according to that temperature (see www.hydro.washington.edu/Lettenmaier/Models/VIC/Overview/SnowBandsText.shtml).

The infiltration into the top-most soil layers is controlled by the variable infiltration capacity (VIC) curve. The VIC model also features a nonlinear mechanism for simulating slow (baseflow) runoff response, and explicit treatment of vegetation effects on the surface energy balance. In the VIC model, water can only enter a grid cell via the atmosphere. Grid cells are simulated independently of each other and once water reaches the channel network, it is assumed to stay in the channel and cannot flow back into the soil. The routing of runoff into streams is

performed separately from the land surface simulation. As of yet, we do not include runoff routing in our implementation since we currently do not have forcing data for the entire CRB.

The model parameters were calibrated as part of a recent study on climate change impacts on the Columbia River basin. In short, a series of streamflow observations were inversely routed (Pan and Wood, 2013) to the grid cell level. These series were used to calibrate each grid cell independently. For a more detailed description of the calibration procedures, see chapter 3.2.3 of this thesis.

Model spin-up is the time taken for the internal states of the model (i.e. soil moisture) to reach a state of equilibrium from an initial state (e.g. Yang et al., 1995, Rahman et al., 2016). Our model spin-up was accomplished by first running the model (from an initial state) for years 1979-2015 and saving the final hydrologic state. The model was then re-started and run for five years, 1979-1984. From the final state of that run, the model was started in 1979 and run until present and hydrological fluxes and states were archived at a daily time step.

VIC 5 allows for exact restarts, which means that running the model for a certain period in one simulation gives the same results as running the model for that period in shorter fragments, given that each run is started with the state file generated in the previous run. This is useful in a real-time system as described here, since a spin up period is not required every day. However, a two month run is required each day to account for updates in the meteorological dataset that is used to force the hydrologic model (described in section 2.2.3). Continuously carrying forward the hydrologic state from the previous run, the current hydrological state is the result of an extended simulation starting in 1979.

2.2.3 Meteorological data

We use meteorological forcing data from a publicly available archive created by our collaborators at the University of Idaho (Abatzoglou, 2013). The archive contains daily surface meteorological data for the Continental United States at 1/24th degree resolution for the time period of 1979 to present, updated daily with a lag of 2 days. The dataset was created by combining temporal attributes of regional-scale reanalysis, gauge-based precipitation from NLDAS-2 and spatial attributes of gridded climate data from PRISM (Abatzoglou, 2013). The dataset includes a number of meteorological variables. The variables we use as forcings for

running VIC are maximum and minimum temperature, precipitation, wind speed, surface downwelling shortwave radiation and specific humidity.

The dataset is updated daily with the latest data typically available by 1 PM PST. The data for the previous 60 days are preliminary. Each day, we therefore download the previous 61 days to account for any updates in the dataset. The hydrologic model is run for this whole period, saving the state after the first day. The next day's run uses this state as an initial state.

The meterorological data is regridded from a resolution of $1/24^{th}$ degree to $1/16^{th}$ degree to match our hydrologic model setup, using CDO (Climate Data Operators; Available at www.mpimet.mpg.de/cdo). The daily fields are disaggregated into 3-hourly using a disaggregating scheme embedded in VIC (in versions prior to VIC 5.0, see www.hydro.washington.edu/Lettenmaier/Models/VIC/Documentation/VICDisagg.shtml).

Other meteorological variables that VIC requires (and are not part of the University of Idaho dataset) include downwelling longwave radiation, atmospheric pressure and density. VIC's meteorological preprocessor estimates longwave radiation using the Prata (1996) algorithm and calculates atmospheric pressure and density from grid cell elevation and global mean pressure lapse rates.

2.2.4 Calculation of percentiles

Different hydrological models have different representations of soil components and snow algorithms. Reporting absolute values of soil moisture or SWE might therefore be misleading. By using percentiles with respect to a historic simulation performed using the same model to report soil moisture states and snow conditions, we ensure that a consistent comparison is being made.

In our system, the percentiles are calculated with reference to a fixed 30 year reference period, calendar years 1981-2010. We adopted the same scheme of calculating the percentiles from the UW Surface Water Monitor system. An empirical CDF is generated for a particular day of the year by collecting VIC output data for five days around that day (the two previous days, current day, and the two subsequent days) for all years within the reference period, for all grid cells in the domain. This results in 150 historical values for each day of the year. These values are ranked and the Weibull plotting position is used to create an empirical CDF. The Weibull

plotting position for the rth ranked (from largest to smallest) value from n historic values is obtained using the equation

$$q_r = \frac{r}{n+1}$$

In real time, the current day's values are transformed into percentiles using linear interpolation between the two closest plotting position values. If a given day's value falls outside the historic range, special measures are needed. We assign a fixed percentile value in these cases, q_{low} if the current day's value is lower than any value in the reference period and q_{high} if the current day's value is higher than any historic value, as given by the following equations.

$$q_{min} = \frac{\frac{1}{(n+1)}}{2} \qquad q_{low} = \frac{1}{(n+1)} - q_{min} \qquad q_{high} = \frac{n}{(n+1)} + q_{min}$$

Figure 2.3 illustrates how percentiles are calculated for given grid cell in the domain.

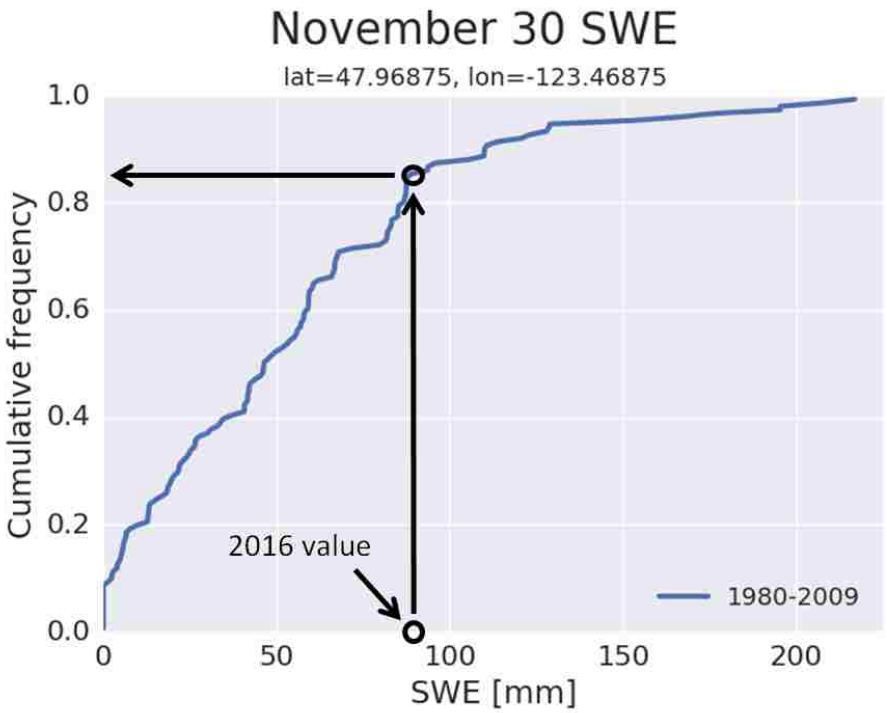

Figure 2.3: An example of how percentiles for hydrologic conditions are calculated in the NW Climate Toolbox. The figure shows ranked November 30th SWE at one grid cell for the historic period 1981-2010, plotted against the Weibull plotting position. The annotation explains how the simulated SWE value of 2016 was given a percentile value.

When plotting SWE percentiles, we exclude grid cells that contain less than 10 mm of SWE if the historic mean at the given grid cell for that day is also less than 10 mm.
During leap years, February 29 percentiles are calculated with reference to the historic values of February 28 to avoid inconsistency in the length of the historic reference period.

2.2.5 Computational description

The current version of the system described here runs on a single CPU of a LINUX workstation (OS version StackIQ Rocks+ 6.01 on AMD Opteron 6238 x2, 2600 MHz 12C x2 CPUs, 64 GB RAM). The ecFlow workflow management software (ECMWF, 2015) is used to run the operational suites. EcFlow is a workflow package, developed at the European Centre for Medium-Range Weather Forecasts (ECMWF), which allows users to run many interdependent

programs in a controlled environment. EcFlow submits tasks and receives acknowledgements when the tasks change status (ECMWF, 2015).

All scripts used by the system are under version control on GitHub (www.github.com/UW-Hydro/monitor).

2.2.6 Workflow

The workflow of the hydrologic components of the NW Climate Toolbox is described in figure 2.4.

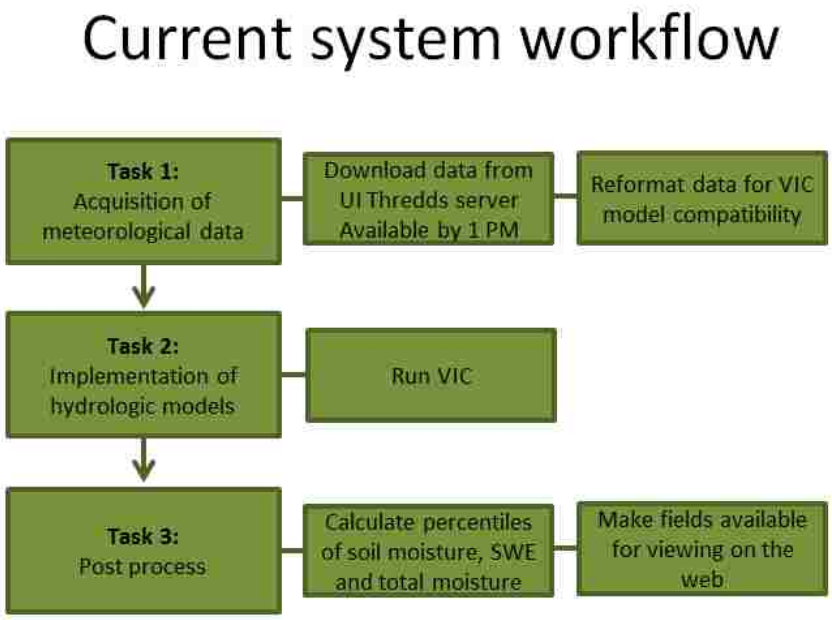

Figure 2.4: A diagram showing the current system workflow of the hydrologic components of the NW Climate Toolbox.

The monitoring process is scheduled to start when the meteorological dataset has been updated at approximately 13:30 p.m. PST. The first task is the acquisition of the meteorological forcing data. The data is downloaded from the University of Idaho via a threads server. The data is then re-gridded from 1/24th degree resolution to 1/16th to match our hydrologic model setup. The daily fields are then disaggregated to a 3-hourly timestep and the additional variables needed by VIC are calculated. VIC is then run for 61 days as described earlier.

After running VIC, a series of post-processing steps are carried through. For the most recent day, percentiles are calculated for soil moisture, SWE and total moisture as described in

section 2.2.4. Three separate netCDF files are generated containing percentiles for each variable and these files are transferred to a shared space where our collaborators at the University of Idaho can access them. As soon as the files have been transferred, they are posted on the webpage (www.nwclimatetoolbox.weebly.com).

2.3 Current hydrologic products on the NW Climate Toolbox website

As for now, the model-derived hydrologic variables available on the NW Climate Toolbox website are percentiles for SWE, soil moisture (SM) and total moisture (TM) which is the sum of SWE and SM. Figures 2.5-2.7 show examples of the percentile plots on the website.

Figure 2.5 shows the design of the NW Climate Toolbox website design (set up by Katherine Hegewisch, University of Idaho). In the topmost panel, users can choose variables to view in a drop down menu. They can also change the map layout and graphics and download the data in a netCDF format. On this figure, SWE percentiles for 2016/12/02 are shown.

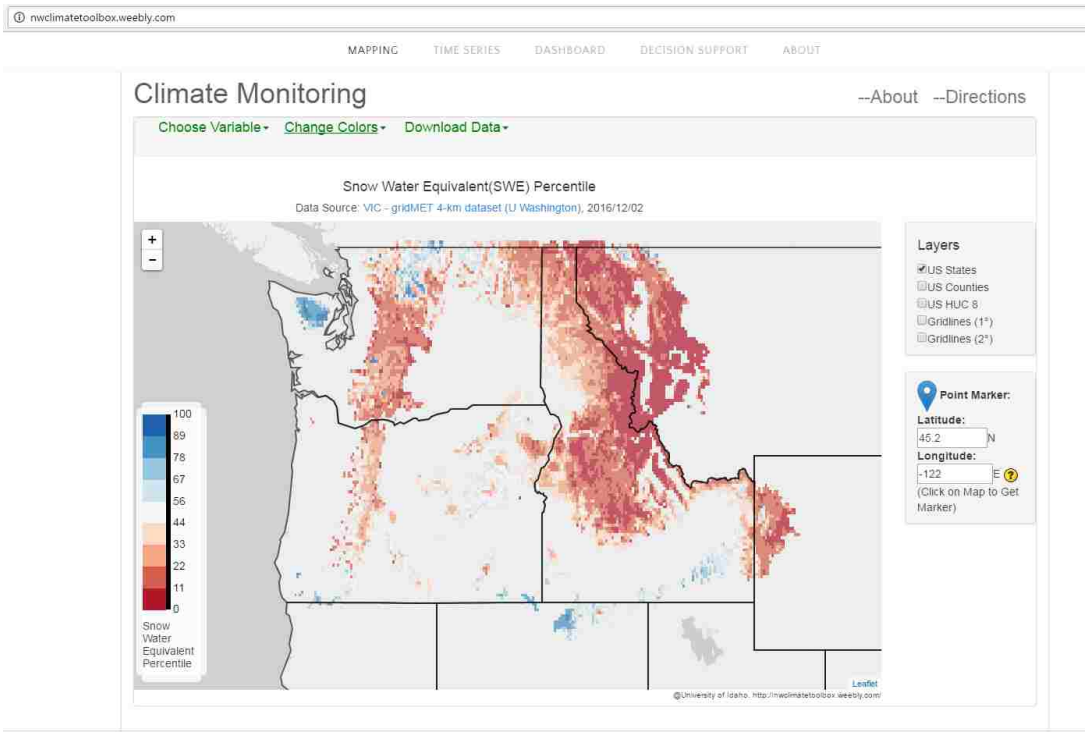

Figure 2.5: The NW Climate Toolbox Website (www.nwclimatetoolbox.weebly.com). The map shows snow water equivalent percentiles for 2016/12/02.

In figure 2.6, soil moisture percentiles for the same day are shown. A single grid cell has been selected and its percentile value is displayed. The users can also pan and zoom the map freely.

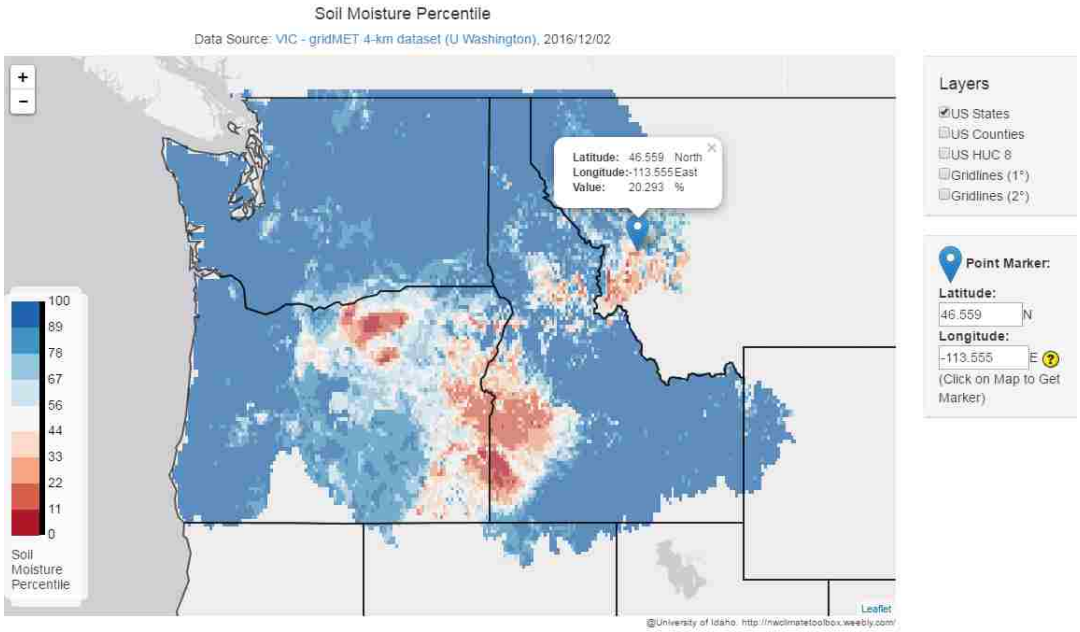

Figure 2.6: Soil moisture percentiles for 2016/12/02 as shown by the NW Climate Toolbox. A single grid cell has been selected and its percentile value is displayed.

In figure 2.7, total moisture percentiles are shown. The underlying map has been changed to a satellite image.

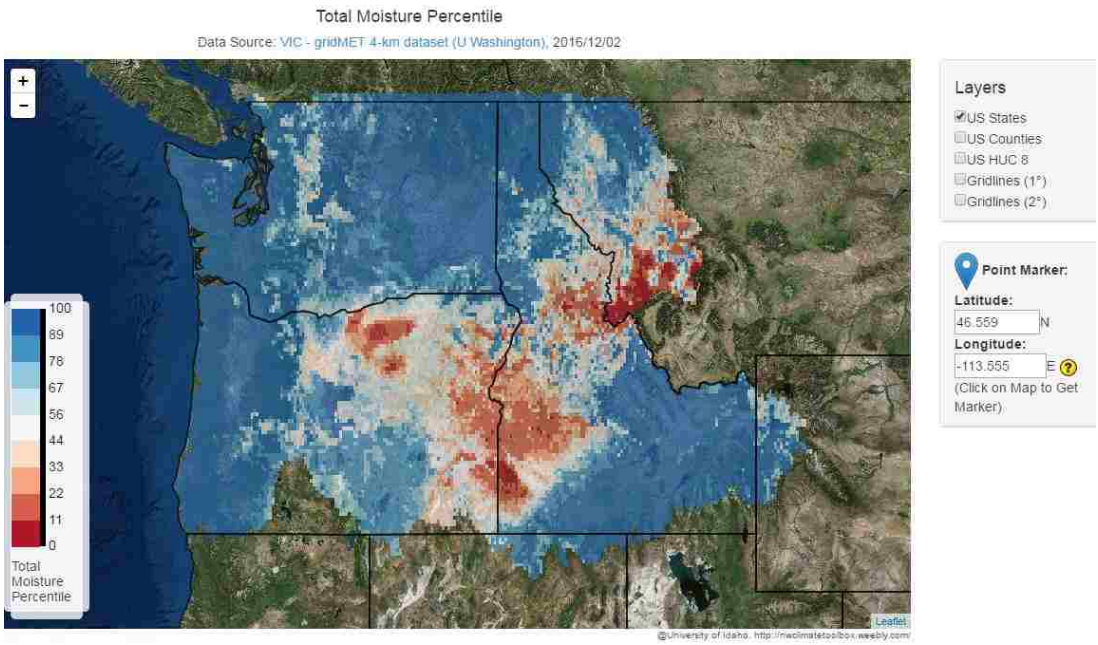

Figure 2.7: Total moisture percentiles for 2016/12/02 as shown by the NW Climate Toolbox. The underlying map has been changed to a satellite image.

2.4 Moving forward

Numerous opportunities exist when it comes to moving forward with the work described in this chapter. Seasonal forecasts from the National Multi-Model Ensemble (NMME; Kirtman et al., 2014), already incorporated in the NW Climate Toolbox, can be used to produce seasonal hydrological forecasts of hydrologic states and fluxes. Also, once meteorological forcings for the full CRB have been incorporated, this initial version of the NW Climate Toolbox can be expanded to include routed streamflow and stream temperature at locations of interest. Outputs from future model runs based on climate model projections can be added to the Toolbox framework to contextualize the projected change in climate in the 21st century in the region. An example of this is illustrated in chapter 3.4. Lastly, the ongoing research into drought monitoring and drought information systems can be merged with ongoing research into next generation hydrologic models which are designed to evaluate hydrologic uncertainty.

Integrating all this into the NW Climate Toolbox will require the development of new graphics and interactive tools to ensure that the information will be easily accessible by users. Along the way, stakeholder input and feedback needs to be solicited to ensure that the NW Toolbox will be a useful tool in resource management in the PNW.

3. Future projections of snow conditions in the Pacific Northwest

3.1 Introduction

Largely induced by economic and population growth, anthropogenic greenhouse gas (GHG) emissions since the pre-industrial era have driven atmospheric GHG concentrations to levels unprecedented in at least the last 800,000 years (IPCC, 2014). Less efficient energy loss from the climate system has resulted in a globally averaged temperature increase of 0.85°C over the period 1880-2012 (IPCC, 2014). One of the most pronounced effects of climate change is the loss of snow cover and the melting of the world's glaciers. Trend analysis shows that northern hemisphere snow cover has undergone severe reductions over the past ~90 years and the rate has accelerated over the past 40 years (Brown and Robinson, 2011). Over the period 1970-2010, the extent of Northern Hemisphere March and April snow cover decreased by 7% and 11% respectively from pre-1970 values (Brown and Robinson, 2011).

Understanding the effects of climate change at regional scales is important to support local decision-making and planning in water resources. Changes in temperature, snow accumulation and river flows that are consistent with expected human-caused trends have been detected in the North American Pacific Northwest (PNW) (Dalton et al., 2013). Mote et al (2010) concluded that annually averaged temperature in the PNW increased by approximately 0.8°C in the 20th century. At the same time, precipitation increased by 13-38% (Mote et al. 2003a) and these changes have already had apparent effects on snow accumulation in the region (Mote et al. 2003b).

The Columbia River Basin (CRB) is highly developed and managed, mainly for hydropower production, flood control, irrigation, fisheries and ecosystem services, navigation and recreation. Over 250 major dams and 100 large hydropower projects are managed within the basin (Payne et al., 2004). The Columbia River has 29 gigawatts (GW) of installed hydroelectric generating capacity and generates a large part of the total hydroelectricity in the United States. The Columbia River is subject to severe floods and one of the original purposes for many of the dams that have been built on the river was mitigating flood risk (BPA, 2001). Flood control remains a high priority for system operations, particularly along the lower river near Portland, OR.

Most of the annual precipitation in the Columbia River Basin occurs during the winter

months, of which the largest share falls in the mountains as snow. The hydrology of the CRB is therefore dominated by the cycle of snow accumulation and melt. Water that is stored in snow during the winter is released when it melts in the spring and summer. About 60% of the natural runoff in the basin occurs during May, June and July (BPA, 2001). Figure 3.1 shows the annual pattern of flow at The Dalles, OR.

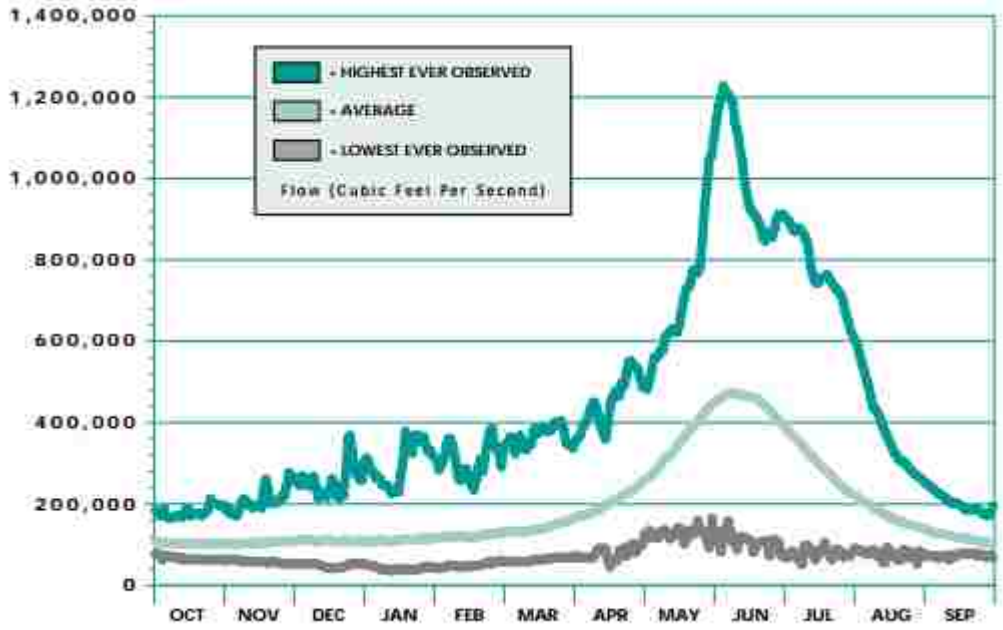

Figure 3.1: Discharge in the Columbia River at the Dalles, OR (Figure source: BPA, 2001).

The figure shows how the discharge peaks in the spring and early summer as a result of the melting snowpack upstream. The figure also shows why flood control is one of the top priorities in the management of the river, with the highest flow ever observed reaching almost three times the historic average.

The shift in the hydrologic cycle caused by less mountain snow is one of the most significant impacts of climate change in the area (Hamlet and Lettenmaier, 1999). Changes in precipitation and increasing air temperatures are predicted to cause a shift in timing of water availability and loss of storage capacity in the region (Dalton et al., 2013). Being able to predict how large these changes will be as the region plans for future water resources associated with hydropower production, flood control, salmon restoration and water supply is invaluable.

Less mountain snow in the region will also affect skiing tourism, which globally has been repeatedly identified as vulnerable to climate change (e.g. Scott and Mills, 2006). Knowing how

climate change might affect the winter snow sports industry in the region is important. In 2009/2010, the industry added $984.9 million in economic value to the states' economy in Washington, Oregon and Idaho alone (Burakowski and Magnusson, 2012). That same winter, the industry supported the employment of 17,089 in these states (Burakowski and Magnusson, 2012).

In this chapter, we examine projected changes in snow conditions in the PNW during the 21st century. For this purpose, we take advantage of a large number of hydrological simulations that have been conducted as part of a new study to evaluate climate change impacts on the hydrology of the Columbia River Basin. The study uses two hydrologic models, forced by ten different global climate models (GCMs) based on two different representative concentration pathways (RCPs) and downscaled using two downscaling methods. The large number of model simulations enables us to improve our understanding of the uncertainty in future snow projections and allows us to evaluate how methodological choices affect the spread in the projections.

First we will analyze temperature and precipitation projections from the climate models. We will then take a closer look at the projected SWE values, focusing on the spread in the model ensemble. We will try to identify areas that exhibit more or less uncertainty in SWE projections. Furthermore, we will look at how the seasonal SWE accumulations are projected to change. We will compare our results to existing research on climate change projections for the PNW.

We also implement novel ways of contextualizing the projected future snow conditions. The 2015 winter was abnormally warm in the western United States which led to a severe snow drought in the region. Records were broken at over 80% of measurement sites west of 115° W in terms of low snow accumulation (Mote et al., 2016). By comparing the recent snow drought year of 2015 to our projections, we are able to contextualize the future snow conditions in an intuitive way for resource managers as well as the general public. Since water managers and policy makers have recently had to deal with a low snow year in the likes of 2015, this is useful in planning efforts for the 21st century since all precautions that needed to be taken are in fresh memory. This could provide water-dependent municipalities and industries in the area with an insight on how they will need to adjust their business structure in the long term.

To offer a practical application, we will also examine the implications of less snow for ski resorts in the region. As mentioned above, the snow sports industry is valuable in the PNW

and to date, little research has been focused on climate change impacts on the industry in the region. We will look at how the number of skiable days at 19 ski resorts in the area is projected to change in the 21st century.

3.2 Domain

Our domain consists of the North-American Pacific Northwest, defined here as the Columbia River Basin (CRB; USGS Hydrologic Region 17 and the Canadian portion of the basin) and the region's coastal drainages (figure 3.2).

Figure 3.2: The North-American Pacific Northwest. The Columbia River basin is shaded (Figure source: Dalton et al., 2013).

The CRB is the 4th largest watershed in North America and the system drains an area the size of the European territory of France. It covers parts of 7 US states, mainly Washington, Oregon, Idaho and Montana (and portions of Wyoming, Utah and Nevada) as well as the Canadian province of British Columbia. The basin is bounded by the Rocky Mountains to the east and north, the Cascade Range to the west and the Great Basin to the south. The Columbia

River originates at Columbia Lake in British Columbia's Rocky Mountains. It flows from Canada into the United States and eventually reaches the Pacific Ocean near Astoria, Oregon.

To better understand the climatology in terms of snow accumulation in the Pacific Northwest, a variety of classification schemes have been used based on variables such as winter temperature (e.g. Hamlet and Lettenmaier, 2007, Gergel et al., in review) or the ratio of peak SWE to winter precipitation (Hamlet et al., 2013). Some classification schemes also take wind speed into account (e.g. Nolin and Daly, 2006). Perhaps the simplest and most intuitive classification scheme is the one based on winter temperature. We follow the example set by Hamlet and Lettenmaier (2007) and categorize our study region by average midwinter (November – March) temperature (T_w) regime. In our categorization, we have three temperature regimes: Snow dominant ($T_w < -6°$ C), snow-rain transient 1 ($-6°C \leq T_w < 0°$ C) and snow-rain transient 2 ($0°C \leq T_w < 5°C$). Figure 3.3 shows the classification for areas within our study domain that historically have hydrologically significant snow accumulation. We define this as areas that had average April 1 SWE greater 10mm during the historic reference period 1980 – 2009.

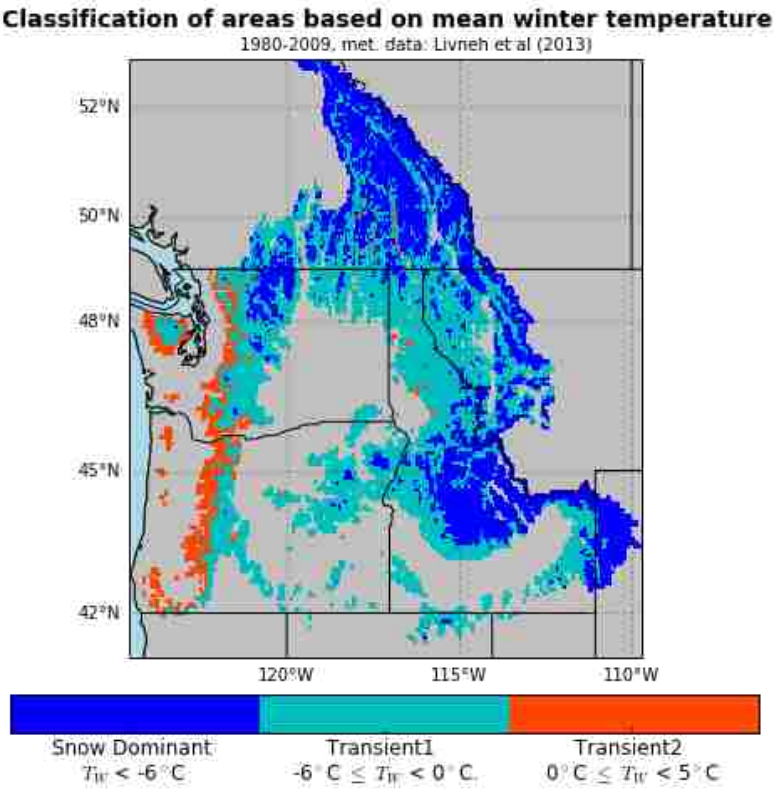

Figure 3.3: Classification of areas based on mean winter temperature 1980 – 2009 as adopted from Hamlet and Lettenmaier (2007). Classification is only shown in areas that historically have hydrologically significant snow accumulation (mean April 1 SWE > 10 mm) as simulated by the VIC hydrologic model (Temperature data source: Livneh et al., 2013).

The figure shows that a large part of the western side of the Olympics and the Cascades classifies as warmer snow-rain transient 2. Higher elevated areas in the central Olympics and Cascades fall into the colder snow-rain transient class 1. Areas in the North-Cascades, the northern (Canadian) part of the basin and the southern Rockies fall into the snow dominant regime.

3.3 Overview of previous climate impacts studies for the Columbia River Basin

The impacts of climate change on water resources in the PNW have been widely acknowledged in recent years. While annually averaged temperatures in the PNW have increased (e.g. Mote et al., 2010), declines in April 1 SWE have been measured at mountain snow course sites of the western US since the mid-20th century. At a majority of locations, considerable declines in SWE coincide with warming, particularly below about 1800 m (Mote, 2003b).

Furthermore, changes in streamflow timing (e.g. Stewart et al., 2005) due to earlier snow melt have been noted.

Several future climate change studies have been conducted for the Columbia River Basin. Since 1990, the Intergovernmental Panel on Climate Change (IPCC) has produced five assessments of the state of climate change science. The Coupled Model Intercomparison Project (CMIP) began in 1995 with the goal to enhance understanding of processes and simulation capacities in global coupled models (Taylor et al., 2011). The last two phases of CMIP, CMIP3 and CMIP5, have been coordinated with the fourth and fifth IPCC assessment reports, AR4 and AR5. In each CMIP dataset, climate change scenarios from Global Climate models (GCMs) are made available for researchers to conduct climate change assessments on regional scales. Since the late 1990s, researchers have been using projections from the CMIP datasets to study climate change implications over the Columbia River Basin, often by coupling a physically based hydrologic model to downscaled climate scenarios. For example, GCM projections from the second IPCC assessment (1995) were used by Miles et al. (2000) to study climate change implications over the Columbia River Basin. Other climate change studies on the CRB and its sub-basins followed (e.g. Cohen et al, 2000; Hamlet, 2003; Payne et al., 2004; Hamlet and Lettenmaier, 2003; Fitzgerald and Burges, 2009; Vano et al., 2010).

The third phase of the Coupled Model Intercomparison Project (CMIP3; Meehl et al., 2007) included a range of scenarios for future GHG emissions. A selection of 10 GCMs from the dataset was used in a comprehensive climate change study on the Columbia River Basin by the UW Climate Impacts Group (Climate Change Scenarios Project, e.g. Hamlet et al., 2010). The study findings showed widespread reductions in April 1 snow as well as a systematic shift in the classification of watersheds from transitional (defined as ratio of peak SWE to Oct-Mar precipitation between 0.1 and 0.4) to rain dominant (ratio less than 1) by the end of the century. The largest changes in snowpack were projected for relatively warm coastal mountain ranges, such as the Cascade Range, and at moderate elevations in the Rockies. On the other hand, the coldest areas in the northern tip of the CRB showed little sensitivity to temperature increases on the order of 2-3°C. The average winter temperature (DJF) in this region is around -10°C so a warming of this magnitude in the 2020s and 2040s has little effect on snow accumulation during that period. These areas therefore only responded to projected changes in precipitation until late in the 21st century, and some areas showed small increases in SWE until the mid-century.

The fifth phase of the Climate Model Intercomparison Project (CMIP5; Taylor et al., 2011) was released in 2011. In this phase, four scenario runs (Representative Concentration Pathways, RCPs) are included based on possible future GHG emissions. Gergel et al. (in review) used climate projections based on the dataset to evaluate climate change impacts on mountain snowpack, soil moisture and dead fuel moisture. They used 10 GCMs and two RCPs to force the VIC model through the 21st century. They found that for all mountain ranges in the western United States, April 1 SWE losses were statistically significant for both GHG emission scenarios. The reductions in SWE in the Rockies (48%, approx. between 42°N and 49°N, i.e. the part of the Rockies that is included in our domain south of the Canadian border) were substantially lower than for the Cascades (65%). Furthermore, they found that the relative spread in their projections was high in parts of the Cascades and the Rockies. Luce et al. (2014) concluded that the interior parts of the Northern Rockies are cold enough to be relatively insensitive to warming, but are instead strongly sensitive to precipitation variation. Luce (2016) concluded that relatively large increases in precipitation could counter the effects of warming on snowpack loss in the Greater Yellowstone Area.

Nolin and Daly (2006) used a data-driven, climatological approach of snow cover classification to map "at risk" snow areas in the PNW, i.e., which snow-dominated winter precipitation areas in the PNW would convert to a rain-dominated area given a 2°C increase in mean winter temperature. For a rain/snow threshold of 0°C, they found that these "at risk" areas covered 9200 km^2 which, given an average 68.4 cm annual peak SWE (computed from 11 SNOTEL sites within these areas), corresponds to a loss in SWE storage of approximately 6.5 km^3 of water. They also found that many areas in the PNW would see an increase in the number of warm winters (defined as a winter whose average monthly temperatures exceed the rain/snow threshold for at least one month of the DJF period), with these impacts concentrated in the Cascade and Olympic ranges. Because of this, a number of lower elevation ski areas could experience negative impacts.

Casola et al. (2005) looked at how ski conditions at three ski areas in the Cascades, Stevens Pass, Snoqualmie Pass and Mission Ridge, would be affected by climate change. They found that impacts increase with a decrease in the elevation of the ski area and a corresponding increase in temperature. Given a 2°C warming, which was projected to occur around the 2020s by a selection of models from the CMIP3 dataset, ski season length could reduce by 14-28% for

Stevens Pass and Snoqualmie Pass and the percentage of rainy days during the season could increase by 50%. Furthermore, they found that the higher elevated Mission Ridge would not be significantly affected. An extension of this study (Hamlet et al., unpublished) underlined the dependence of location in regards to severity of climate change impacts of ski resorts in the region. Analyzing 21 ski resorts in diverse locations and at a range of elevations both east and west of the Cascades, they found that the ski areas most sensitive to warming were the ones influenced by the maritime climate west of the Cascades and at moderate elevations. Further research on climate change impacts for ski areas in the PNW has not been conducted to the author's knowledge. Climate change impacts have been much more investigated for ski areas in northeastern United States (e.g. Scott and Mills, 2006, Scott et al., 2007, Dawson et al., 2009) and Canada (e.g. Scott et al., 2007). Scott et al. (2007) found that the projected loss of natural snowpack will have significant negative impacts on the snowmobile industry in the northeastern US. However, when it comes to the ski industry, a large investment in snowmaking could substantially reduce the negative effects of climate warming. Historically, ski areas in the PNW have invested less money in snowmaking and are thus more vulnerable to fluctuations in natural snowfall (Burakowski and Magnusson, 2012).

3.4 Methods

3.4.1 Study overview and analysis period

Our study is an update and extension to the Columbia Basin Climate Change Scenarios Project (CBCCSP), a study on the effects of climate change on the CRB by the University of Washington Climate Impacts Group (see section 3.3). We analyze the hydrological output from two hydrologic models, forced by ten different global climate models (GCMs) and two different representative concentration pathways (RCPs), resulting in 80 individual simulations in total. There are several updates and new features from the 2010 CBCCSP project. We use climate projections from the CMIP5 dataset (see section 3.3) downscaled using two downscaling methods on a finer temporal scale. A new calibration technique (see section 3.2.3) is implemented using data from more sites in the basin. The final products consist of daily streamflow sequences from all individual simulations at 388 sites in the basin (as opposed to 297) as well as spatial fields for hydrologically-relevant variables.

A period of 30 years is often used as climatology in climate studies. We partitioned the simulations into four consecutive 30-year periods: historical (1980-2009), early-century (2010-2039), mid-century (2040-2069) and late-century (2070-2099). These periods were chosen to have comparable results to previous studies (e.g. Hamlet et al., 2013). From here on, these periods will be referred to as 1990s, 2020s, 2050s and 2080s, respectively. We evaluate projected hydrologic changes using these periods throughout the study.

3.4.2 Climate projections

Rupp et al. (2013) compared 41 GCMs from the CMIP5 suite to observations in the PNW for the 20th century. Using a set of metrics, focusing on the models' ability to reproduce historic temperature and precipitation, they evaluated models by overall performance. The information was used in this study to select 10 GCMs from the CMIP5 experiments based on their PNW performance to force two hydrologic models under two GHG emission scenarios (RCP 4.5 and 8.5) through the 21st century. The output from climate models needs to be corrected for biases, and is too coarse to be used for basin-scale hydrologic analysis. Before it can be used to force a hydrologic model, it therefore requires spatial downscaling and bias correction. Downscaling can be done via dynamical or statistical methods. The main disadvantages of dynamic downscaling are that they do not incorporate bias correction and it is computationally demanding, which makes it impractical for simulations on a long timescale using multiple emission scenarios and CGMs, as used in this study. On the other hand, statistical downscaling is computationally efficient and easy to use. Two statistical downscaling methods, Bias-Corrected Spatial Disaggregation (BCSD, Wood et al., 2002) and Multivariate Adaptive Constructed Analogs (MACA, Abatzoglou et al., 2012) were therefore used in this study to relate the large scale climate features from the GCMs to a 1/16th degree resolution over the PNW.

Meteorological inputs used as the training dataset for the BCSD and MACA downscaling were taken from Livneh et al (2013).

3.4.3 Hydrologic modeling

The output from the GCMs was used to force two hydrologic models, the Variable Infiltration Capacity model (VIC; Liang et al., 1994, version 4.2.glacier, available at www.

github.com/UW-Hydro/VIC/tree/support/VIC.4.2.glacier) and the Precipitation Runoff Modeling System (PRMS; Leavesley et al., 1983, version 3.0.5). These models were implemented at 1/16th degree scale (~6 km) across the Pacific Northwest. Both models have been widely used in regional climate change impact studies around the world (e.g. Elsner et. al, 2010, Steele et al, 2010). For a detailed description of the VIC hydrologic model, see section 2.2. of this thesis.

VIC uses a sub-daily (3-hour time step in our case) snow model. Figure 3.4 illustrates the dominant processes in this snow model.

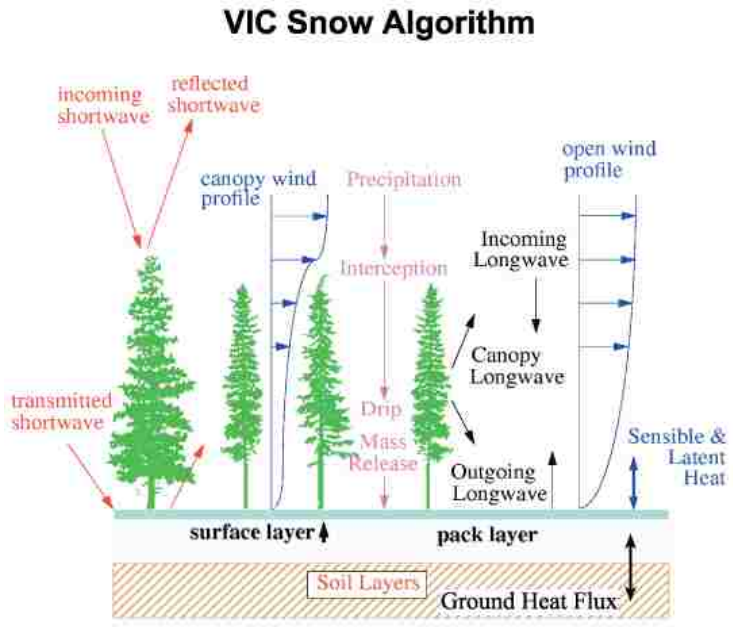

Figure 3.4: The VIC snow model explained (Figure source: Andreadis et al., 2009).

In our implementation, VIC considers snow in the forms of ground snow pack and snow in the vegetation canopy. The model uses a two-layer representation of the snow pack. The upper snow layer is used to solve the energy balance at the snow pack surface (Andreadis et al, 2009). The model partitions precipitation into rain and snow and snowfall is added to the snowpack. If the energy balance is positive melt will occur and if it is negative, an iteration is performed on the surface temperature to solve the balance. Melted snow or excess liquid water is released as snowpack outflow. A novel glacier representation is embedded in this version of the VIC hydrologic model. The model uses a simple ice volume to area scaling relationship to mimic the effects of glacier dynamics and turns snow into ice based on a density threshold (Hamman et al.,

2014). This keeps SWE from accumulating from year to year in grid cells that are cold and receive ample precipitation.

Figure 3.5 illustrates how snow processes are represented in the PRMS model.

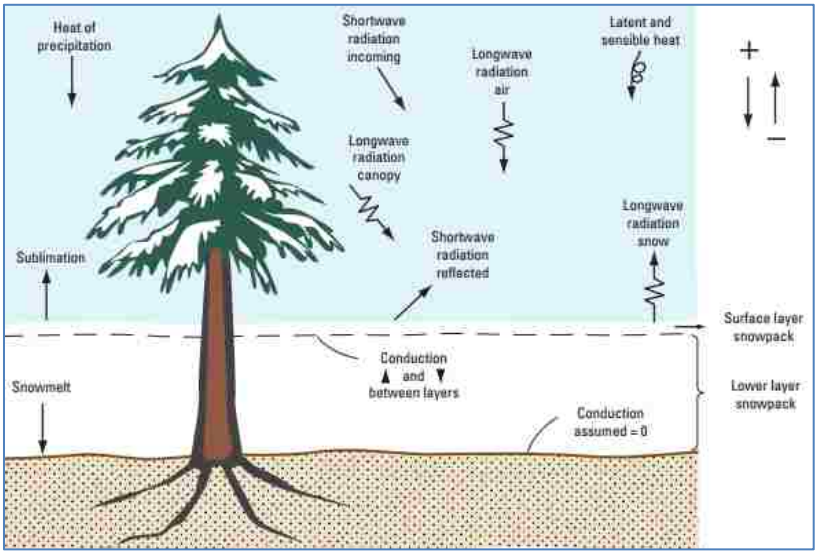

Figure 3.5: The PRMS snow module explained. Components of the snowpack energy balance, accumulation, snowmelt and sublimation are shown (Figure source: Markstrom et al., 2015).

The PRMS model simulates the commencement, accumulation and ablation of a snowpack in each grid cell. The dynamics of the snowpack are simulated through estimates of water and energy balances. The conservation of these entities ensures that the difference between inputs and outputs is equal to the change in snowpack storage. Energy can be exchanged between the snowpack and the atmosphere in both directions through radiation, conduction, or convection, and the surface layer is considered separately for solving the energy balance at the surface (as in VIC). Precipitation will also affect energy storage if it occurs at a temperature other than freezing (Markstrom et al., 2015). The albedo is simulated separately to determine how much radiation is reflected, and the snowpack density is simulated to estimate the thermal conductivity of the snowpack. The ability of plants to intercept and sublimate snow is a function of the plant-cover type. As in VIC, grass cannot intercept snow as it is assumed to be buried beneath it. Shrubs and trees will intercept snow (Markstrom et al., 2015).

The PRMS model contains no glacier component to prevent SWE from accumulating from year to year. Instead, in our implementation, all SWE is simply removed at the end of each water year. Also, PRMS does not contain elevation bands as VIC does (see chapter 2.2.2).

The models were calibrated using a no-regulation, no-irrigation (NRNI) flow time series at ~180 discrete locations throughout the CRB. The NRNI dataset excludes any effects from humans on streamflow in order to replicate natural flow in the river. This streamflow dataset was provided by the River Management Joint Operating Committee, a multi-agency organization comprised of the Bonneville Power Administration, the United States Army Corps of Engineers and the United States Bureau of Reclamation.

For model calibration purposes, the NRNI streamflow observations were disaggregated using an inverse flow routing scheme (Pan and Wood, 2013) into spatially-distributed runoff fields at a daily time step. Using these fields, each model grid cell was calibrated independently using the Kling-Gupta Efficiency (KGE) as the objective function. The KGE was calculated on a weekly time step to minimize the effects of timing errors in the disaggregated runoff fields. The advantage of this calibration method over the traditional calibration at discrete points along a river network is that sharp gradients in calibrated parameters between neighboring subbasins are avoided.

3.4.4 Contextualizing future snow conditions

The 2015 snow season set records for many locations in the western United States (Mote et al., 2016). Although precipitation was only slightly below normal, abnormally warm temperatures during the winter months led to record low snow accumulations. Figure 3.6 shows percentiles of maximum SWE of the 2015 water year as simulated by the VIC hydrologic model, using meteorological forcings from the University of Idaho (Abatzoglou, 2012). Percentiles were calculated with reference to the 1990s. Values that fall outside of the historic range (below the range in this case) are assigned percentile values in accordance with section 2.2.4.

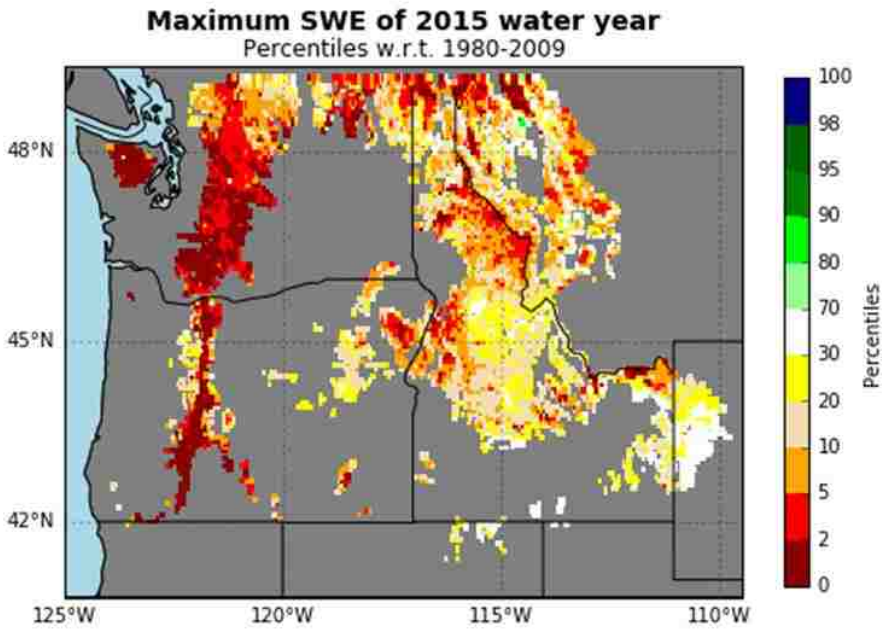

Figure 3.6: Percentiles of maximum SWE of the 2015 water year as simulated by the VIC hydrologic model. Percentiles were calculated with reference to the historic period 1980 – 2009. Atmospheric forcings are from Abatzoglou, 2012.

Figure 3.6 shows that in the Olympic Mountains and in a large part of the Cascades, the yearly maximum SWE of 2015 was within the 5th percentile of the historic period. Percentile values in the Rocky Mountains were a little bit higher, although maximum SWE values for most regions did not exceed the 30th percentile of the historic period. In Wyoming, the maximum SWE percentiles were in the 30-70 range.

Figure 3.7 shows March 1, 2015, SWE percentiles as reported by the Natural Resources Conservation Service snow measurement sites.

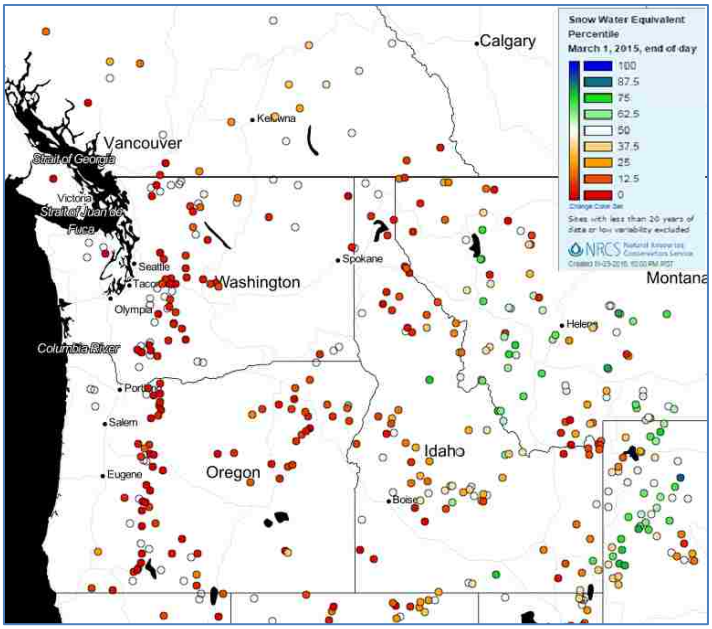

Figure 3.7: Percentiles of March 1st SWE of 2015 as reported by the Natural Resources Conservation Service snow measurement sites. Sites with less than 20 years of data or low variability are excluded.

Again, we see that the Cascades had low snow accumulations. The snow conditions in the Olympic Mountains are not as bad as depicted by figure 3.6, and several sites in the Rockies and in Wyoming report higher than average SWE at this time. Still, the overall message from those two figures is that for the Pacific Northwest in general, the 2015 snow year was abnormally low.

As discussed in section 3.1, temperature increases are projected for the PNW in the 21st century. Using our future snow simulations, we investigate how exceptional or common the snow accumulations from a low snow year like the 2015 will be in the future.

We do this by examining how the distribution of annual maximum SWE changes. We extract 30 year periods every ten years between 1980 and 2099. We find the future period in which a currently considered a low snow season will be the "normal" season. We define this as the future period during which the SWE value that is equivalent to the 10th percentile during the 1990s becomes larger than or equal to the 50th percentile. This is demonstrated in Figure 3.8, which shows the shift in the probability distribution of annual maximum SWE at Hurricane Ridge, WA, as projected by one GCM, RCP 8.5, and VIC.

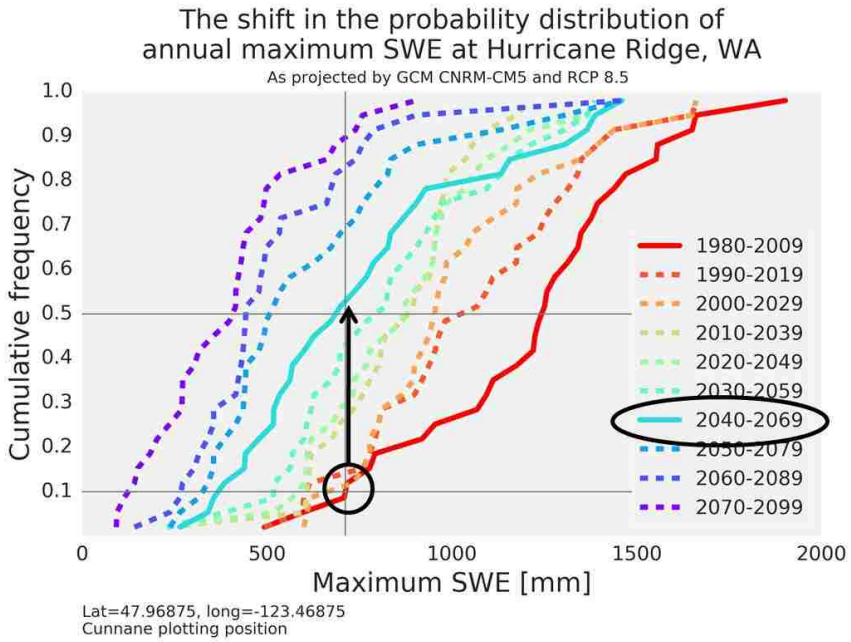

Figure 3.8: The shift in the probability distribution of annual maximum SWE at Hurricane Ridge, Washington.

We find the first future period in which the 10th percentile during the 1990s becomes equal to or larger than the 50th percentile. In this case, we see that for the 2050s the 10th percentile of the historic period has become larger than the 50th percentile. We therefore say that according to these simulations the historically-low SWE becomes normal in the 2050s.

3.4.5 Impacts on ski resorts

When analyzing climate change impacts on ski resorts, authors have used a variety of metrics. Some of these metrics are simple, for example based on projected temperature and precipitation. Nolin and Daly (2006) used a data-driven, climatological approach to compute the relative frequency of winters at selected ski areas with a mean temperature less than a specified temperature threshold. Casola et al. (2005) used three metrics based on hydrological model output, forced by two global climate models. These metrics were the number of days the ski area was open per ski season (based on a minimum SWE value), the percentage of years the ski area had opened at December 1 and the percentage of days during the ski season that it rained.

Examples of more complicated metrics also exist in the literature, even incorporating adaption efforts such as snow making into the climate change impact assessment (e.g. Scott et al. 2003, 2006, 2007; Scott and Jones 2005; Hennessy et al., 2003).

We adapt the climatic criteria defining an operational ski day from Scott et al. (2003). Their criteria were derived from an examination of 17 years of daily ski operations data from ski areas in Ontario and communications with stakeholders in the ski industry. Also, consultations with stakeholders from the Québec ski industry (Bourque and Scott 2004) and the Vermont ski industry (Scott 2004) affirmed that these criteria were generally transferable to these areas. As defined in Scott et al. 2003, we will assume ski areas will close if any one of the following conditions occurs: snow depth went below 30 cm, two-day liquid precipitation exceeded 20 mm or maximum daily temperature exceeded 15ºC. We will also assume the same fixed snow density of 220 kg/m^3 to relate SWE values to snow depth. We use daily SWE and liquid precipitation fields from our hydrologic simulations and daily temperature data as downscaled from the 10 GCMs. Data for each ski area corresponds to the data for the grid cell in which the main lodge is located. We use the general indicator that ski businesses need 100 skiable days per winter to remain profitable. This measure has frequently been used in the literature (e.g. König and Abegg 1997; Elsasser and Bürki 2002, Scott et al., 2007).

Although several socio-economic and business factors also influence ski area operations (e.g. key tourism periods, snow making capacities; e.g. Scott et al., 2006), these factors are beyond the scope of our study.

We analyze climate change impacts at 16 ski resorts that Hamlet et al. (unpublished) chose to look at. These resorts represent a range of locations both east and west of the Cascades as well as a range of elevations. A few of these areas are equipped with snow making capabilities. The locations of these ski areas are shown in figure 3.9. The location of each ski area corresponds to the center of the grid cell in which the main lodge is located. The ski areas and the mean elevation in the corresponding grid cell are listed in table 1.

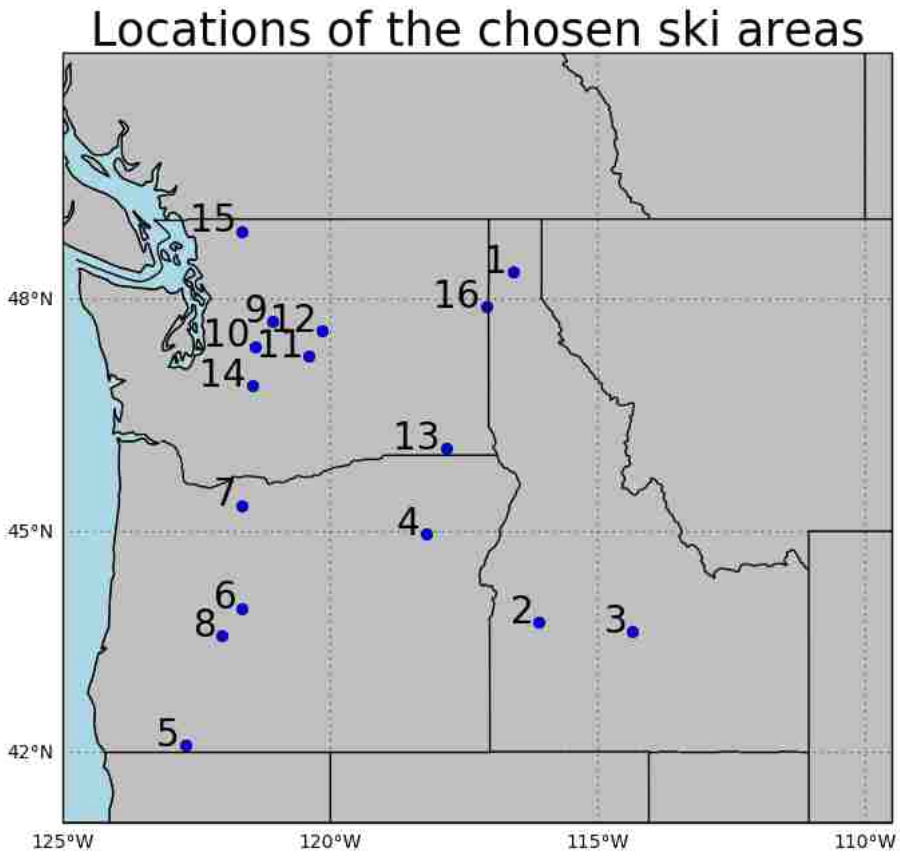

Figure 3.9: The locations of the ski areas that were chosen for this analysis.

Table 1: The ski areas analyzed in this study (adopted from Hamlet et al., unpublished).

ID #	Name	Elevation (m)
1	Schweitzer Mountain Resort	1115
2	Bogus Basin	1844
3	Sun Valley	1887
4	Anthony Lakes	2144
5	Mt. Ashland	1631
6	Mt. Bachelor	2015
7	Mt. Hood Meadows	1875
8	Willamette Pass	1613
9	Stevens Pass	1363
10	The Summit at Snoqualmie	1034
11	Mission Ridge	1655
12	Badger Mt.	1033
13	Bluewood Ski Area	1456
14	Crystal Mt.	1556
15	Mt. Baker	1186
16	Mt. Spokane	1308

3.5 Results

3.5.1 Temperature and precipitation projections

Figure 3.10 shows the average change in winter (DJF) temperature between the 1990s and the 2050s and 2080s over the CRB and coastal drainages as projected by the ten GCMs (downscaled using the MACA technique, see Appendix 1 for BCSD) and both RCPs.

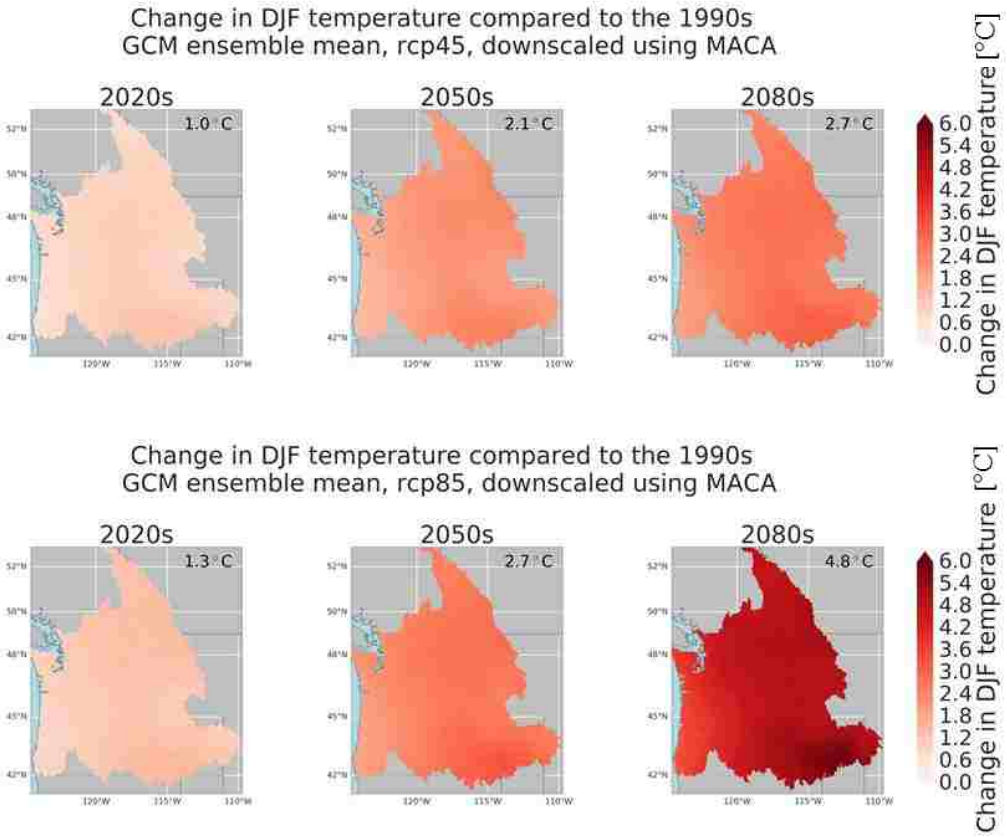

Figure 3.10: Winter temperature change projections for the Columbia River Basin and coastal drainages (GCM ensemble mean, downscaled using MACA).

As expected, RCP 4.5 and 8.5 look similar until the mid-century, projecting an average increase of 2.1°C and 2.7°C, respectively. In the 2080s, we see that RCP 8.5 projects a warming of 4.8°C, which is almost double the warming projected by RCP 4.5 (2.7°C). In general, the models project greater warming as we move from the Pacific Coast towards the inland regions. Also, we see that temperature increases seem relatively high in the southern tip of the basin (southern Idaho and Oregon). Comparing the projections downscaled by BCSD (Appendix 1: Figure A.1.1), we see that the results from the two downscaling methods are almost identical, the

only difference being that the BCSD method results in a slightly lower increase by the 2080s for RCP 4.5 (2.6°C).

Figure 3.11 shows the average change in winter (DJF) precipitation between the 1990s and the 2050s and 2080s over the CRB and coastal drainages as projected by the ten GCMs (downscaled using the MACA technique) and both RCPs.

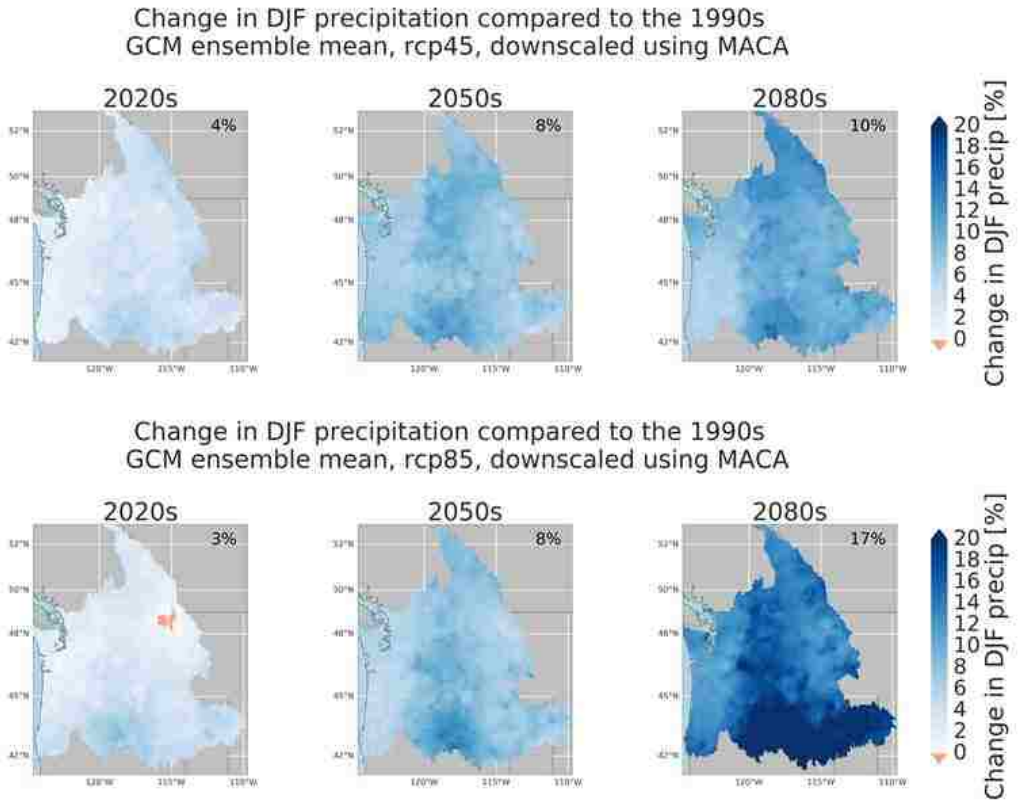

Figure 3.11: Winter precipitation change projections for the Columbia River Basin and coastal drainages for RCP 4.5 and RCP 8.5 (GCM ensemble mean, downscaled using MACA).

Both scenarios predict an overall increase in precipitation for all periods. Again, we see that the two scenarios predict very similar changes up until the 2050s. The most difference between RCP 4.5 and 8.5 is in the 2080s, where the projected increases are 10% and 17%, respectively. We also see that for RCP 8.5, precipitation increases are exceptionally high in southern Idaho and Oregon. The precipitation projections downscaled by BCSD can be seen in Appendix 1 (Figure A.1.2).

Figure 3.12 shows seasonal temperature changes for each GCM averaged over the PNW, between the 1990s and the periods 2020s, 2050s and 2080s. The percent change projected by

each GCM is obtained by comparing the future simulations with the control simulation from the same GCM.

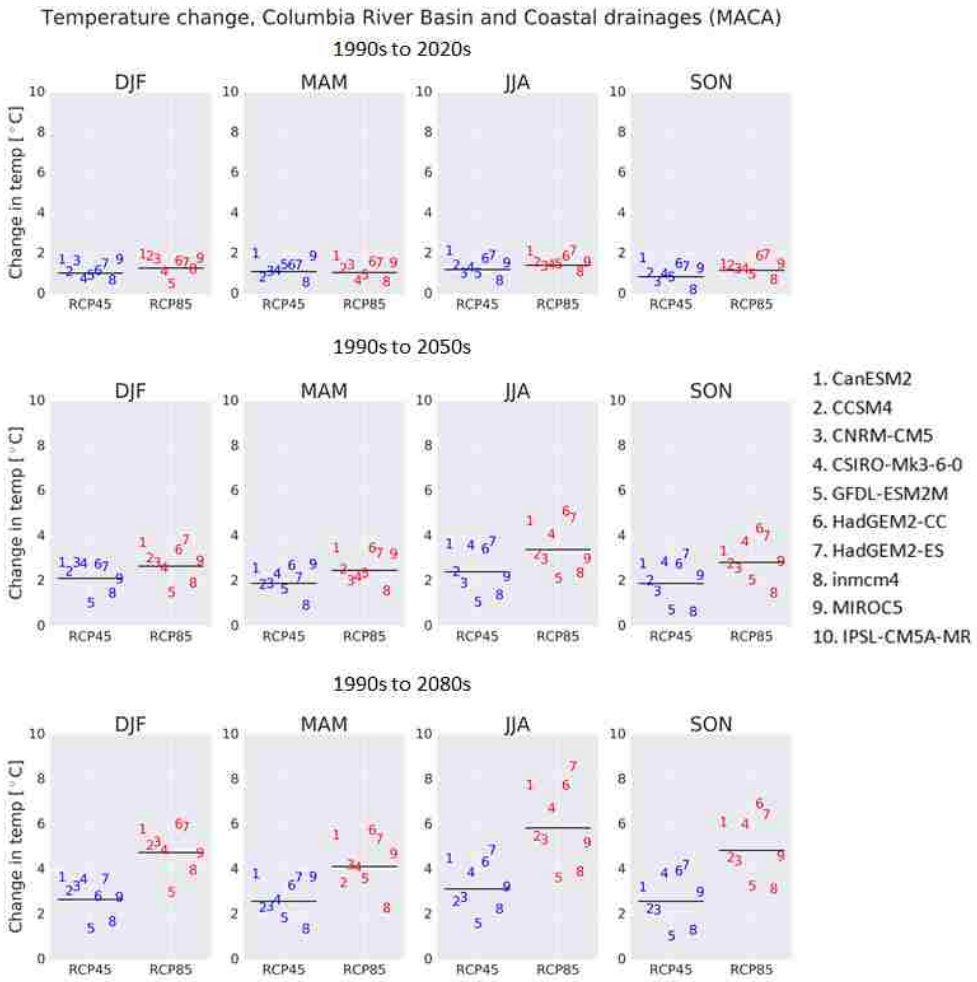

Figure 3.12: Seasonal temperature change projections for the Columbia River Basin and coastal drainages (downscaled using MACA). Blue numbers indicate RCP 4.5 and red numbers indicate RCP 8.5. A horizontal line indicates the corresponding mean.

We see that the spread between GCMs increases from the 2020s to the 2080s, and projected temperature changes are greatest in the summer. We notice that two of the CGMs (GFDL-ESM2M and inmcm4) are consistently much colder than the other models. The GFDL-ESM2M model is especially cold during the winter months. We also notice that for RCP 8.5, the CanESM2, HadGEM2-CC and HadGEM2-CC are usually the warmest three models.

Figure 3.13 shows seasonal precipitation changes for each GCM averaged over the PNW.

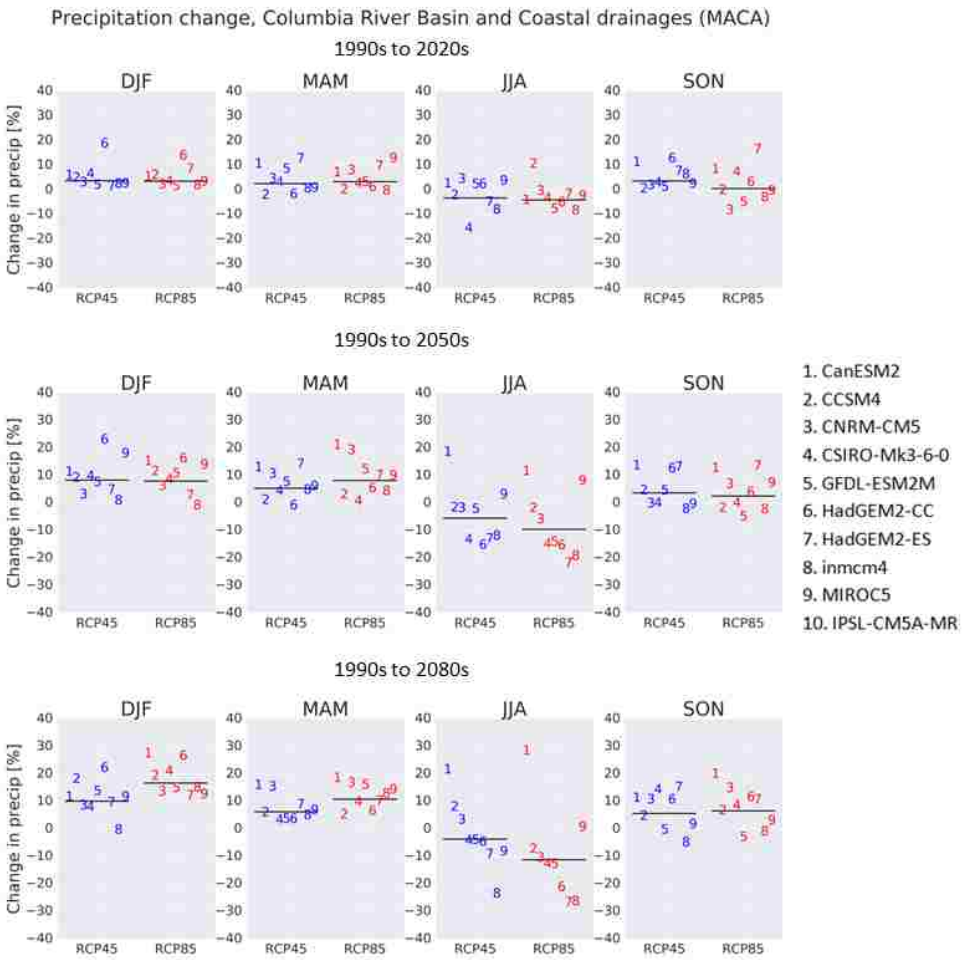

Figure 3.13: Seasonal precipitation change projections for the Columbia River Basin and coastal drainages (downscaled using MACA). Blue numbers indicate RCP 4.5 and red numbers indicate RCP 8.5. A horizontal line indicates the corresponding mean.

The figure shows that all models project precipitation increases over the winter (DJF) months. We see that in general, this applies to the spring and fall months as well. However, a majority of the models project precipitation decreases over the summer. Since summer precipitation is already low in the region, the magnitude of these percentage values might not be comparable to that of the other seasons. For precipitation, we do not notice an increase in the spread between the GCMs between the 2050s and the 2080s and the magnitude of these values is similar. Looking at the two colder models identified above, inmcm4 and GFDL-ESM2M, we notice that the inmcm4 model projects very low winter precipitation increases, especially for the 2080s, and the GFDL-ESM2M model is generally close to the average.

The winter (DJF) temperature and precipitation changes will inherently affect snow accumulations in the region. While winter temperature is projected to increase, so is winter precipitation. This might counteract the effects of warming on snow accumulations in the region to some extent.

3.5.2 Projected changes in snowpack

Figure 3.14 compares the historic annual peak SWE to the ensemble mean projection for the 2080s (for both RCPs and downscaling method BCSD).

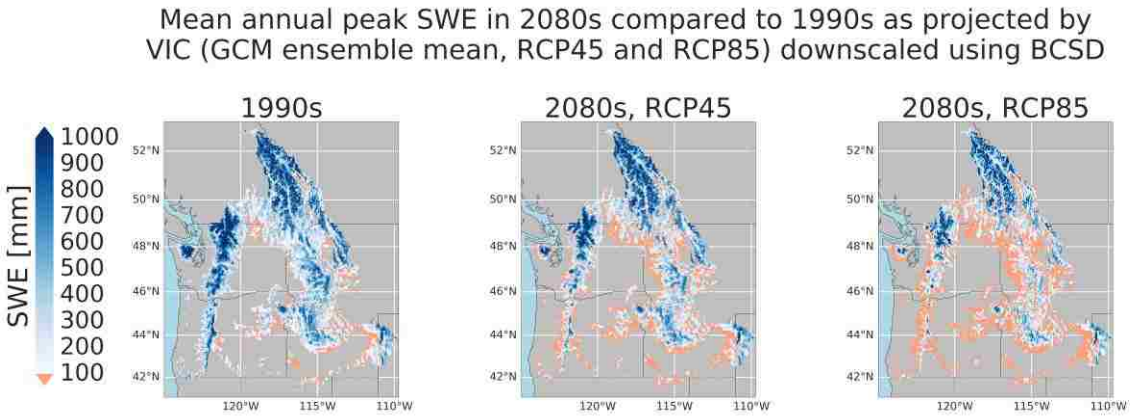

Figure 3.14: Mean annual peak SWE in 2080s compared to 1990s as projected by VIC (GCM ensemble mean) for both RCP 4.5 and 8.5 (downscaled by BCSD downscaling method, see Appendix 2 for outputs from MACA downscaling method and PRMS hydrologic model). Note that grid cells with mean April 1 SWE < 10mm in the historic period are masked out.

As expected, there is more loss of SWE in the warmer scenario (RCP 8.5) where we see a great reduction in the southern Cascades, in the foothills of the Olympics and in eastern Washington and Oregon. The snowpack in the Canadian part of the basin (northern Rockies) seems relatively unaffected for this scenario. We also see an area in the northern Cascades that is relatively unaffected in the 2080s. These are roughly the areas that classify as snow dominant in figure 3.3.

We see the same patterns for RCP 4.5, but generally less decreases in snow. The most significant changes occur in the Olympics and southern Cascades. For this scenario, no significant changes are visible in almost the entire Canadian part of the basin and the northern Cascades. Parts of the southern Rockies also seem intact.

The top panels in figures 3.15 (RCP 4.5) and 3.16 (RCP 8.5) show the percent change in annual peak SWE between the 1990s and the 2020s, 2050s and 2080s for downscaling method BCSD and VIC hydrologic model.

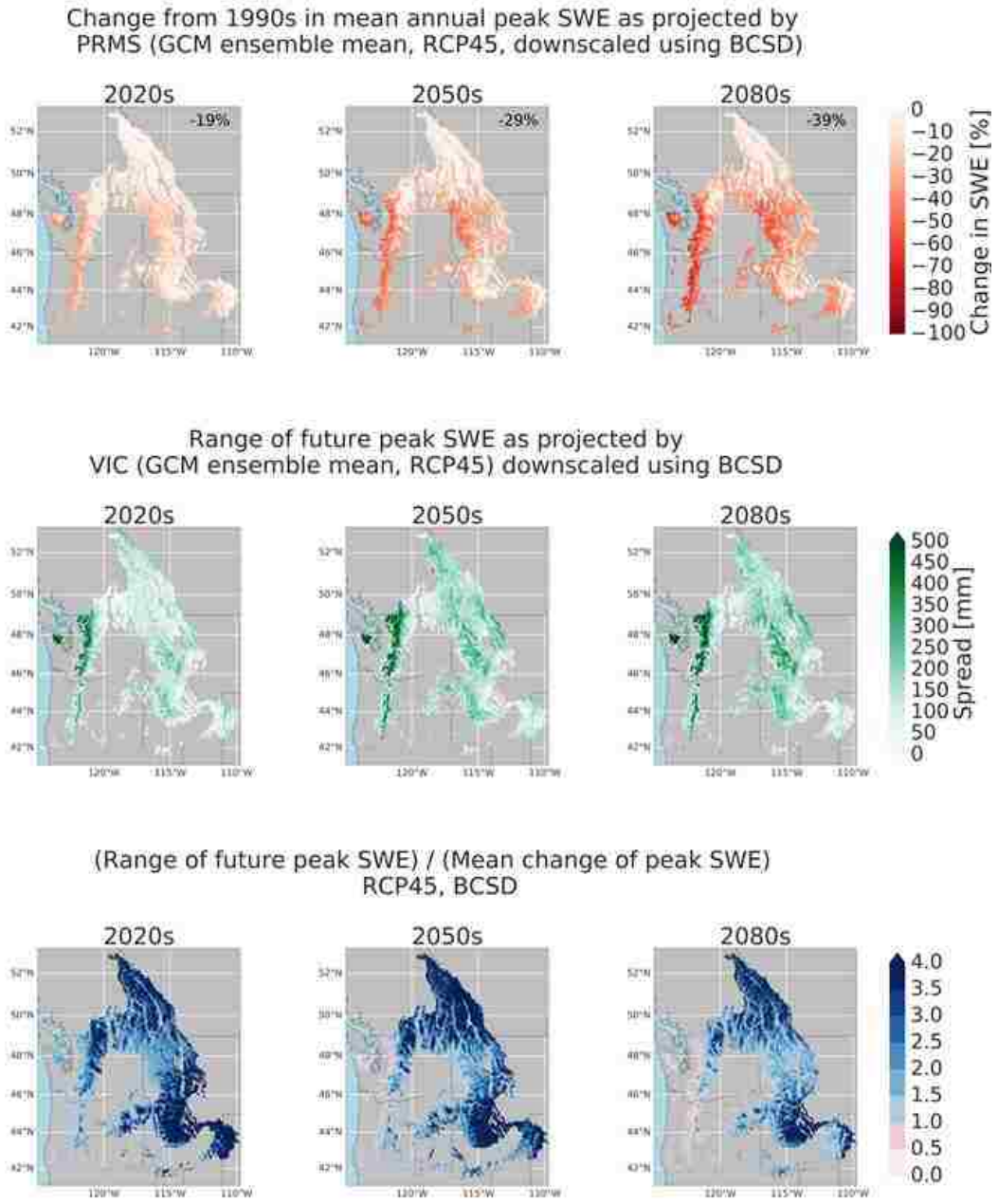

Figure 3.15: Analysis of changes in annual peak SWE as projected by RCP 4.5, VIC, GCM ensemble, downscaled using BCSD. (a) Percent change in annual peak SWE between the 1990s and the 2020s, 2050s and 2080s. (b) Range of future peak SWE within the GCM ensemble. (c) The range of future peak SWE divided by the mean change of peak SWE. Note that grid cells with mean April 1 SWE < 10mm in the historic period are masked out.

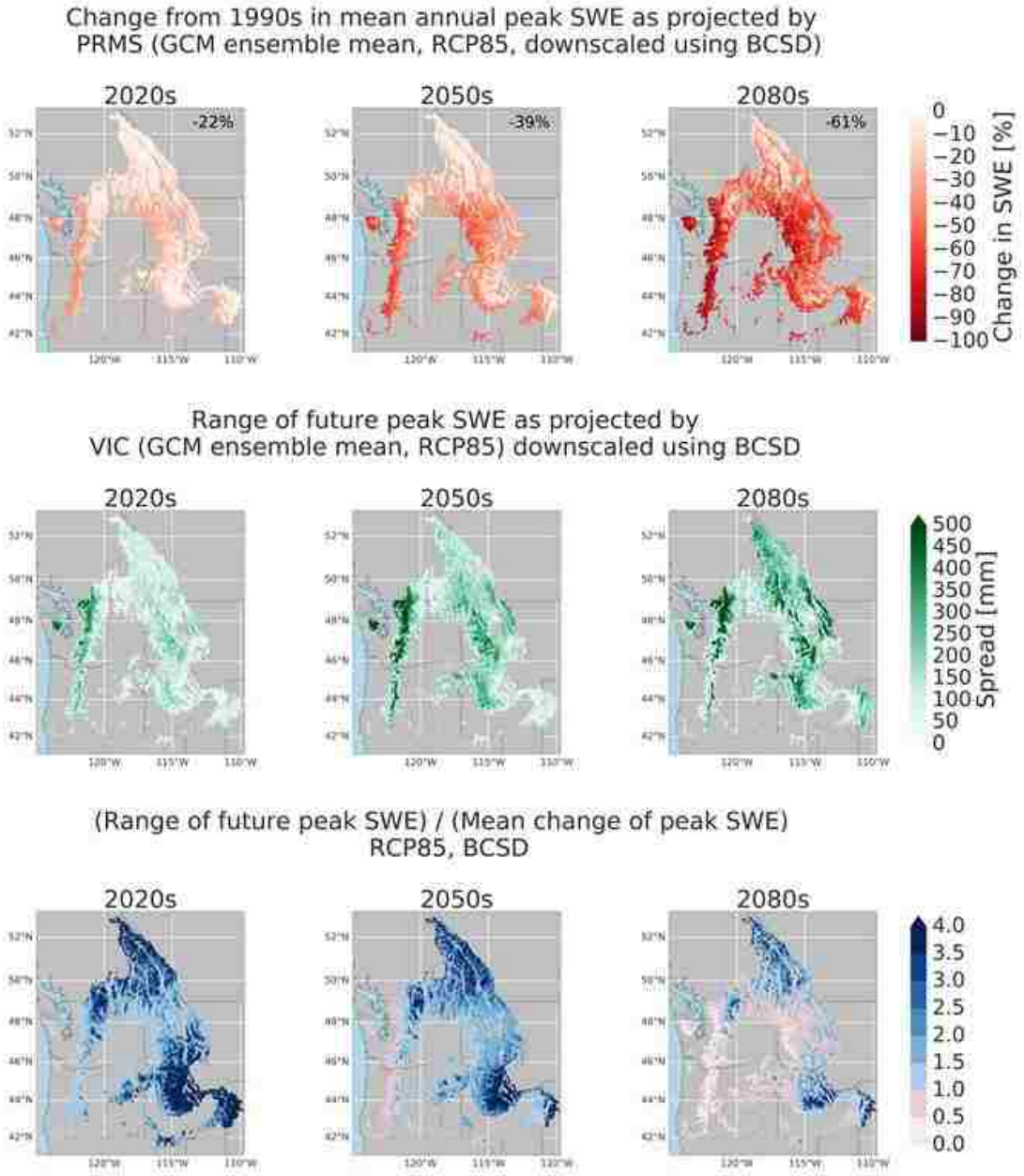

Figure 3.16: Analysis of changes in annual peak SWE as projected by RCP 8.5, VIC, GCM ensemble downscaled using BCSD. (a) Percent change in annual peak SWE between the 1990s and the 2020s, 2050s and 2080s. (b) Range of future peak SWE within the GCM ensemble. (c) The range of future peak SWE divided by the mean change of peak SWE. Note that grid cells with mean April 1 SWE < 10mm in the historic period are masked out.

The mean change across all 10 models is calculated and shown in the figure. The area-averaged decline in annual peak SWE for the 2020s, 2050s and 2080s are 19%, 29%

and 39%, respectively, for RCP 4.5 and 22%, 39% and 61% for RCP 8.5. These differences in the reductions between the two scenarios are quite large, especially in the 2080s (22%)

Figures 3.15 and 3.16 (middle panels) show the spread in annual peak SWE projections (across all ten GCMs) between the historic and future periods. We see that the range in future peak SWE projections is greatest in the Northern Cascades and the Olympics. The range is very similar for RCP 4.5 and 8.5, especially for the first two periods (2020s and 2050s). In the 2080s, a greater range is apparent for RCP 8.5 in the Rocky Mountains.

To summarize this information, the spread in the projections is divided by the mean change in annual peak SWE. This way, we can more easily identify areas in which there is more or less uncertainty in the projections of future snow. A value of 1 from this metric means that the range of peak SWE projections is equal to the mean projected change, and a high (low) value from this metric means that the range of peak SWE projections is higher (lower) than the mean projected change in SWE. Gergel et al. (in review) used this metric for the same purpose, and Luce (2016) used a similar metric based on precipitation and temperature changes.

The summary figure for RCP 4.5 (figure 3.15, bottom panel) shows that the metric takes rather high values in most regions for all periods, except for the Cascades and the Olympics. There, the mean change in annual peak SWE is clearly larger than the spread in the projections for mid- and (especially) late century. The reason for the relatively high values of this metric, at least for the first two periods, is most likely that the mean changes in peak SWE (the denominator) is rather low.

For RCP 8.5 (figure 3.16, bottom panel), we see the same pattern for the 2020s and the 2050s as we saw for the 2050s and 2080s for RCP 4.5. For the 2080s, we see that the mean changes in annual peak SWE have exceeded the range in projections everywhere except in the Northern and Southern Rockies.

Figure 3.17 shows a comparison of this metric between 2050s and 2080s on one hand and BCSD and MACA downscaling methods on the other.

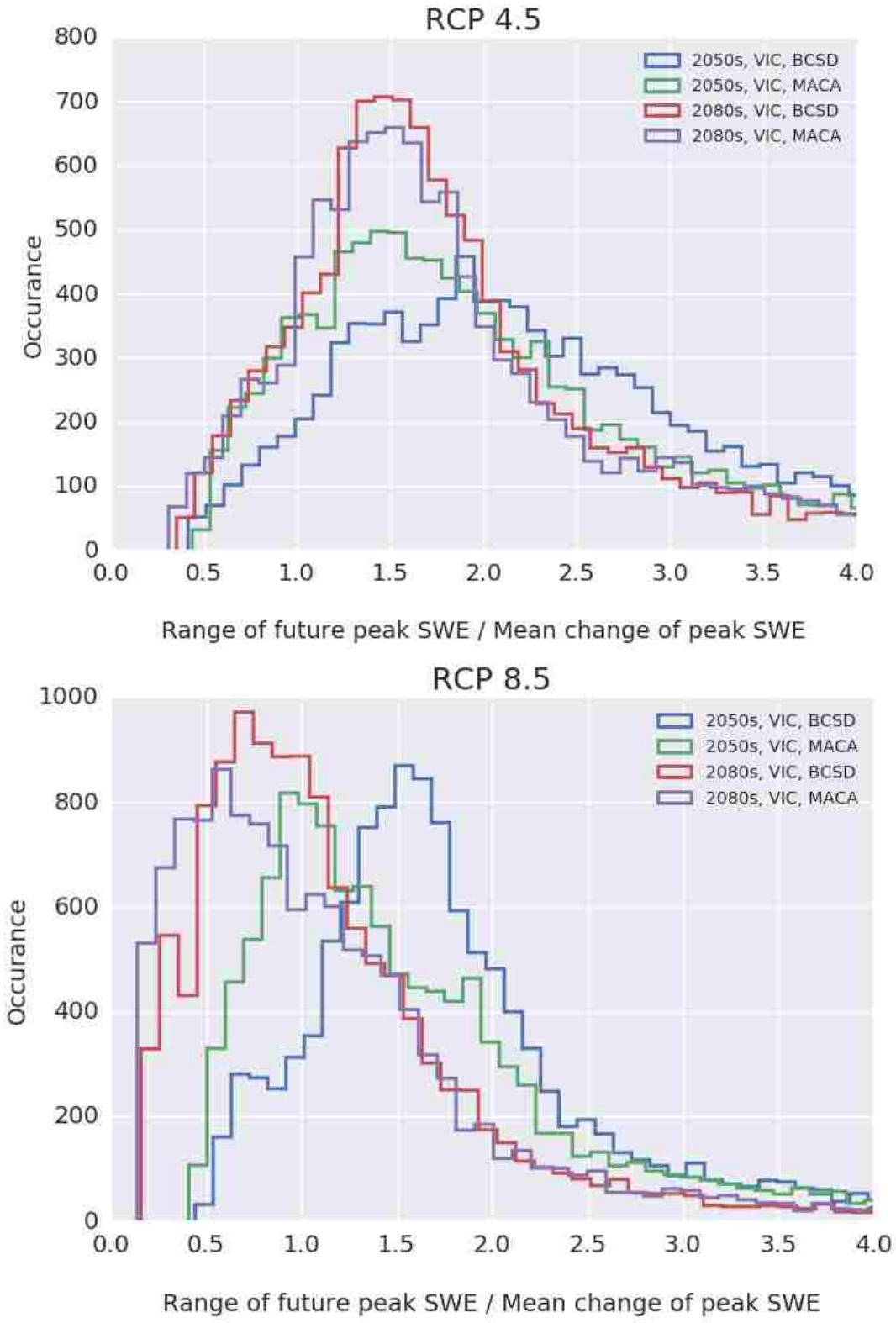

Figure 3.17: A histogram showing the range of future peak SWE divided by the mean change of peak SWE for RCP 4.5 and 8.5, downscaled using MACA and BCSD.

For RCP 4.5, we see that the two downscaling methods are quite similar in the 2080s but differ substantially in the 2050s, with BCSD having a tendency to show higher values for the metric. We see this for RCP 8.5 in both the 2050s and the 2080s as well. This suggests that more uncertainty is associated with BCSD for future peak SWE projections than MACA.

Figure 3.18 shows the annual cycle of volumetric SWE in the PNW (left panel: VIC, right panel: PRMS).

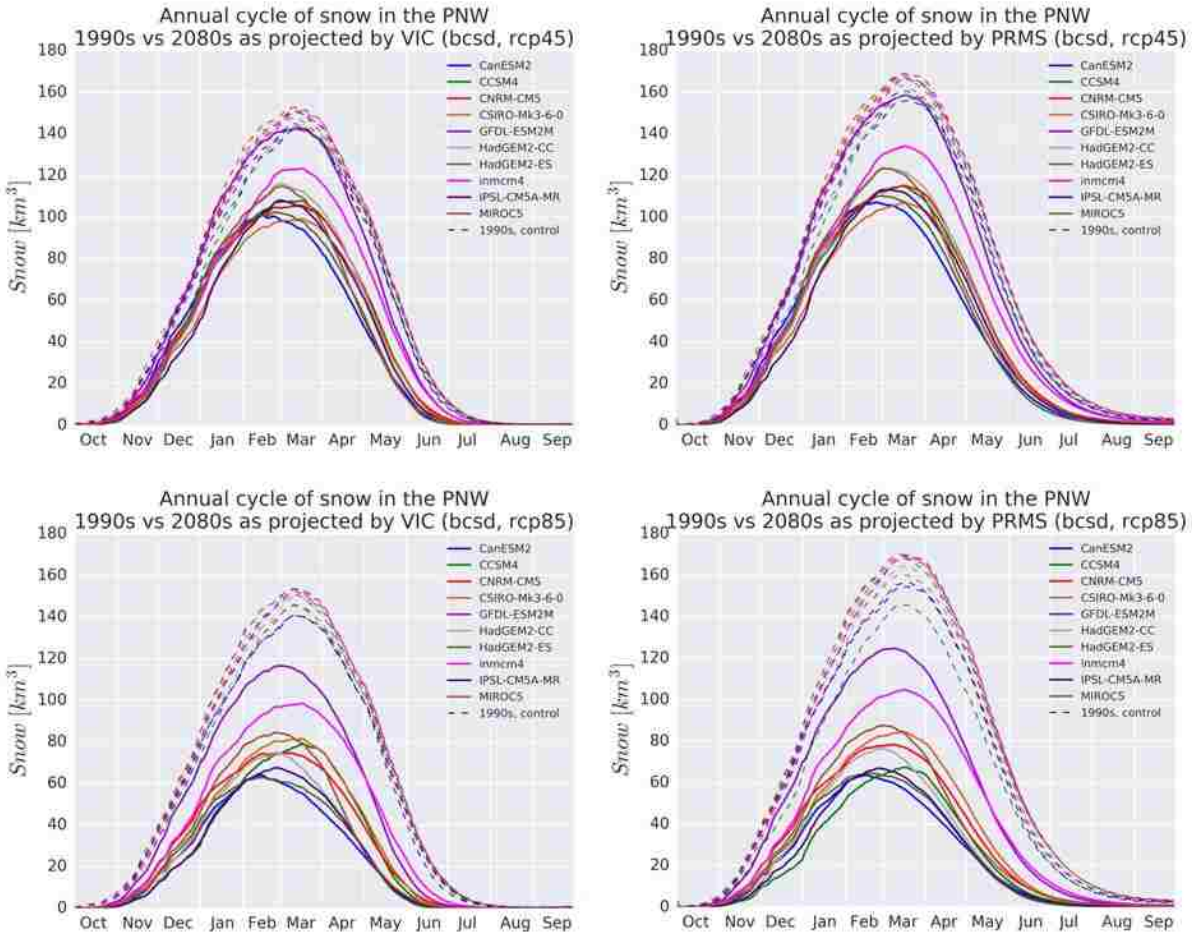

Figure 3.18: The annual cycle of volumetric SWE in the PNW. The 1990s are compared with the 2080s as projected by VIC and PRMS and 10 GCMs (downscaled using BCSD, see Appendix 2 for MACA).

The models that stand out as having a small reduction in SWE volume are the GFDL-ESM2M and the inmcm4, which we identified as the coldest models in section 4.1. For RCP 4.5, volumetric SWE as projected by the GFDL-ESM2M even exceeds the historic values for PRMS and closely resembles the historic values for VIC. The other GCMs project much lower SWE volumes than these two, with a spread of 20-30 km3 at the peak. We also notice that the day of peak basin-wide snow volume seems to move forward by a few weeks in the late century for many of the models (especially for RCP 8.5). The curves thus show a skew to the left, indicating a longer ablation period for the snowpack.

The historic runs from PRMS and VIC are almost identical in terms of seasonal SWE volume. We do however notice that PRMS simulates substantially higher snow volume for RCP 4.5 than does VIC, especially for RCP 4.5 and the control simulations.

3.5.3 Contextualizing future snow conditions

Figure 3.19 shows when the 10^{th} percentile of the annual maximum SWE 1980-2009 becomes the 50^{th}, as projected by VIC and 10 GCMs (downscaled using BCSD).

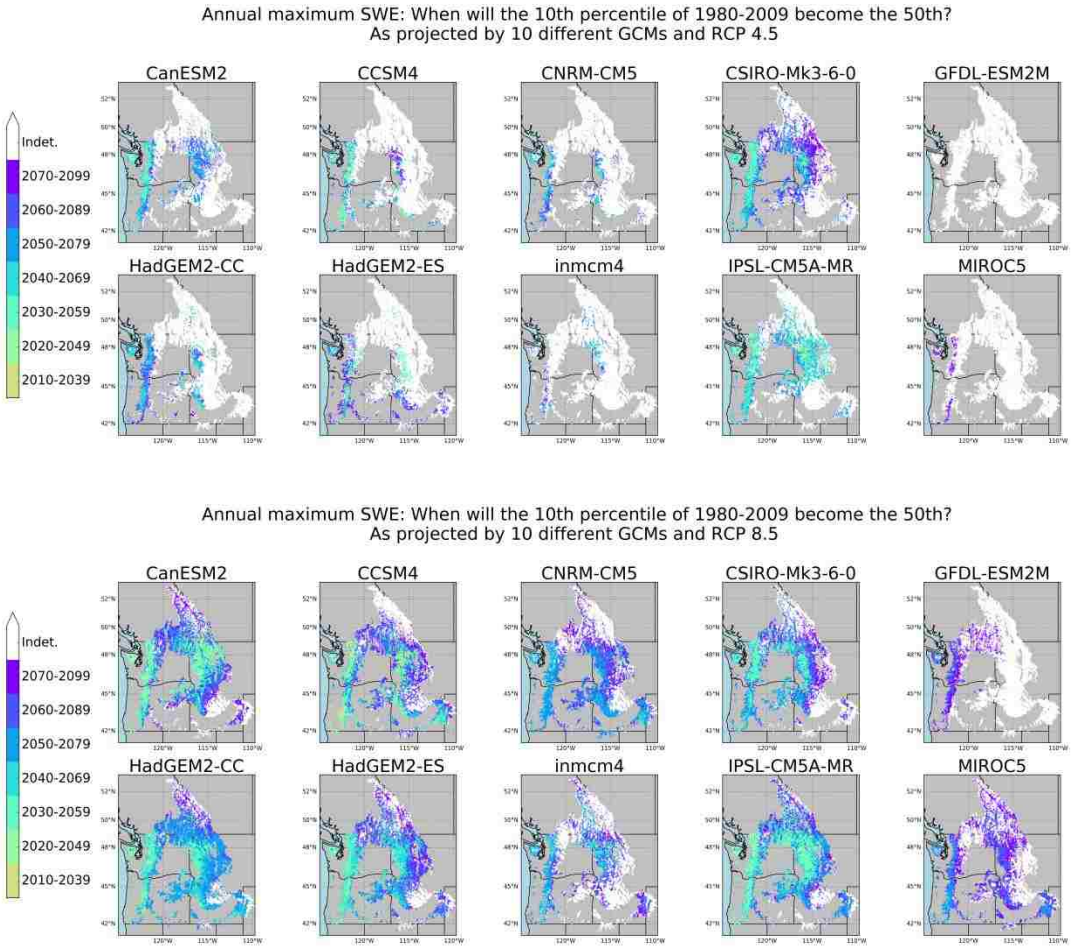

Figure 3.19: Maps of when the 10th percentile of annual maximum SWE 1980-2009 becomes the 50th, as modeled by VIC and the 10 GCMs, downscaled using BCSD. Indeterminate means that the 10th percentile of the 1980s period does not become larger than the 50th percentile for any period before 2100.

For RCP 4.5, much of the North Cascades and the Rocky Mountains will not see the 10th percentile of the 1980s become the average anytime in the 21st century. We do see this happening in the Olympic Mountains and the (western) Cascades for almost all models, where it usually occurs sometime between 2030-2059 and 2050-2089. Again we see that the GFDL-ESM2m and inmcm4 models look particularly cold, and so does the MIROC5 model. The maps for these models are almost completely white, meaning that the 10th percentile of the 1980s will not become commonality anytime during the 21st century.

Looking at the lower panel where results are shown for RCP 8.5, we see that this does occur for a much larger area and sooner than for RCP 4.5. This occurs in the Olympic Mountains and the Cascades for all models, but not much sooner than depicted by RCP 4.5. Most of the

areas in the Rocky Mountains that were shown to be indeterminate for RCP 4.5 now show the 10th percentile of the 1980s becoming the average late in the century. For much of the study domain, including the Rocky Mountains and a part of the northern Cascades, the 10th percentile does not become the norm in the 21st century according to the GFDL-ESM2M model.

3.5.4 Implications for ski resorts in the PNW

Figure 3.20 shows how the length of the ski season is projected to change in 16 ski resorts around the PNW.

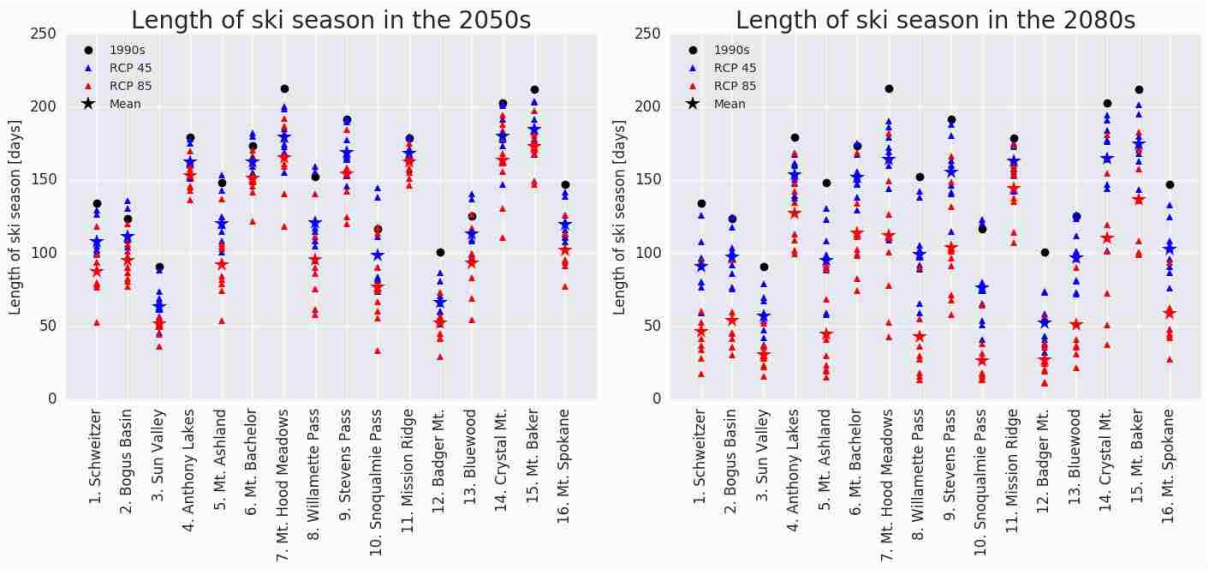

Figure 3.20: Average length of the ski season at 16 ski resorts in the PNW as projected by 10 GCMs (downscaled using MACA) and VIC hydrologic model. Triangles are shown for each GCM simulation for each scenario. A star indicates the mean of these 10 simulations. A blue circle indicates the historic (1990s) average (as forced by Livneh et al., 2013).

Overall, the decrease in skiable days is much larger for RCP 8.5. We also notice that the spread in these results is quite larger for RCP 8.5. The general indicator is that ski resorts need 100 skiable days per season to remain profitable (see section 3.2.5). Assuming that the mean of the GCM ensemble is the most accurate prediction, we can expect 13 of the ski resorts to remain profitable in the 2050s for RCP 4.5 and 8 for RCP 8.5. By the 2080s, these numbers will have decreased to 8 for RCP 4.5 and 7 for RCP 8.5. Here we do not take snow making capabilities into account.

3.6 Discussion

Our projected changes in snowpack over the PNW are generally consistent with previous studies. According to our simulations, declines in snow accumulations will be greatest in the Cascades, especially the southern portion and western slopes, and the Olympics. Higher elevated areas with historic mean winter temperature less than -6°C show more resistance to climate warming. We found that the range in future peak SWE projections is greatest in the northern Cascades and the Olympics. The range in future projections of peak SWE is very similar for RCP 4.5 and 8.5 and increases as we move closer to the end of the century.

We found that two of the GCMs, GFDL-ESM2M and inmcm4, were significantly colder than the other models, resulting in less SWE depletion in the 21st century for these models. The GFDL-ESM2M model projects especially low warming for the winter months, and its projected precipitation increases were average in comparison to the other models. When looking at projected aggregate seasonal SWE, we found that this model projects the largest amount of SWE of all the GCMs. For RCP 4.5, it even projects increases in SWE. While the inmcm4 model also projects relatively cold winter temperatures, its projected precipitation increase is also low, and thus the resulting volumetric SWE projection falls close to the other models. The other eight GCMs generally agree on the magnitude of changes in volumetric SWE.

The choice of downscaling method results in less variability than the choice of hydrological model (Mizukami et al., 2016). We therefore did not expect to see great variation in results between the two downscaling methods. However, our results indicate that the BCSD downscaling method results in higher relative spread for future peak SWE projections than MACA.

More explicit methods are available to obtain a better understanding of the sources of uncertainty in future projections of SWE and perhaps that should be the basis of our further work. For example, Nortrop and Chandler (2014) used a simple statistical model based on Bayesian analysis to partition uncertainty in projections of future climate from multimodel ensembles, both on a global and regional scale. They considered three major sources of uncertainty: the choice of climate model, the choice of emission scenario and the internal variability of the modeled climate system. Their findings were that relative contributions to uncertainty depend on the climate variable under consideration, as well as the region and time horizon.

Climate change impacts for ski resorts in the PNW have not been studied thoroughly in the past. Our analysis shows that the number of skiable days per winter will decrease substantially in the 21st century. There is however a quite large uncertainty between different GCM simulations. Taking the mean of the simulations at each resort, only 8 (RCP 4.5) or 7 (RCP 8.5) resorts (out of 16) will remain profitable in the 2080s if we exclude the mitigating effects of snow making. Further studies should incorporate socio-economic and business decision making factors that also influence ski area operations (e.g. key tourism periods, snow making capacities). Snow making is not as common in ski areas in the PNW as in ski areas in the northeastern US and Canada. In order to stay economically viable by the end of the century, 7 or 8 ski resorts out of the 16 that were studied will need to incorporate snow making. Ample water availability is a key for such procedures.

The author believes that a real-time component of the analysis aimed at contextualizing future snow conditions in section 3.5.3 could be incorporated into the NW Climate Toolbox. In addition to comparing current SWE, soil moisture and total moisture states to historic simulations, we could make comparisons to the future simulations. We would generate empirical cumulative density functions for the future periods as we have already done for the historic period (as described in chapter 2.1) and in real-time we would calculate a plotting position for the current conditions. The user would then be able to choose results from a model ensemble mean or between different GCMs, hydrological models and so on. The author also foresees that at the end of each water year, the user would be able to generate a suite of summary plots that would compare many different snow metrics to the projected future conditions, including annual peak SWE, the length of the snow season, aggregate SWE and so on. This would relate their recent decisions to what they should expect in the future. As stated above, this could be highly useful for water resource managers and policy makers in the region when it comes to long-term planning.

3.7 Conclusions

In this chapter we looked at how snow conditions are projected to change in the 21st century in the PNW. Our findings generally agree with previous studies. Regional warming will result in declining snowpack. The main conclusions of our work are:

- Averaged over the PNW, the GCM ensemble mean indicates that winter temperatures will increase by 2.6°C and 4.8°C for RCP 4.5 and RCP 8.5, respectively, between the 1990s and the 2080s. Similarly, winter precipitation will increase by 10% and 17% (MACA) and 15% and 22% (BCSD). However, summer precipitation is projected to decrease. The increase in winter precipitation might counteract the effects of warming on snow accumulations in the region.
- Declines in snow accumulations will be greatest in the Cascades, especially the southern portion and western slopes, and the Olympics. Higher elevated areas with historic mean winter temperature less than -6 °C show more resistance to climate warming.
- The choice of climate model seems to be the major source of uncertainty in model results. The range in future peak SWE projections between simulations using different climate models is greatest in the northern Cascades and the Olympics.
- Differences in results from the two hydrologic models seem negligible.
- The 10^{th} percentile of the 1990s will become larger than the 50^{th} percentile at varying times across the PNW, depending on climate models and scenarios. In some areas, especially the Canadian part of the Rocky Mountains, this is not projected to occur anytime in the 21^{st} century.
- The number of skiable days in PNW ski areas is projected to decrease substantially in the 21^{st} century. However, there is a large spread in model results so uncertainty is high. No mitigating effects of snow making were included in our analysis and this is something that needs to be incorporated in future studies.

4. References

Abatzoglou, J. T. (2013). Development of gridded surface meteorological data for ecological applications and modelling. *International Journal of Climatology*, *33*(1), 121–131. https://doi.org/10.1002/joc.3413

Abatzoglou, J. T., & Brown, T. J. (2012). A comparison of statistical downscaling methods suited for wildfire applications. *International Journal of Climatology*, *32*(5), 772–780. https://doi.org/10.1002/joc.2312

Bonneville Power Administration (2001). *The Columbia River System Inside Story* (Internal Report - DOE/BP-3372) (p. 78). Retrieved from https://www.bpa.gov/power/pg/columbia_river_inside_story.pdf

Andreadis, K. M., Storck, P., & Lettenmaier, D. P. (2009). Modeling snow accumulation and ablation processes in forested environments: VIC SNOW MODEL. *Water Resources Research*, *45*(5). https://doi.org/10.1029/2008WR007042

Bourque A, Scott D (2004) Future outlook – the effects of climate change on the North American ski industry. Paper presented an the Annual Conference of L'Association des stations de ski du Québec and the Ontario Snow Resort Association, Lac Leamy, Québec1-3 June.

Brown, R. D., & Robinson, D. A. (2011). Northern Hemisphere spring snow cover variability and change over 1922–2010 including an assessment of uncertainty. *The Cryosphere*, *5*(1), 219–229. https://doi.org/10.5194/tc-5-219-2011

Burakowski, E., & Magnusson, M. (2012). *Climate Impacts on the Winter Tourism Economy in the United States*. Retrieved from https://www.nrdc.org/sites/default/files/climate-impacts-winter-tourism-report.pdf

Casola, J. H., Kay, J. E., Snover, A. K., Norheim, R. A., Whitely Binder, L. C., & the Climate Impacts Group (2005). *Climate Impact on Washington's Hydropower, Water Supply, Forests, Fish, and Agriculture*. A report prepared for King County (Washington) by the Climate Impacts Group (Center for Science in the Earth System, Joint Institute for the Study of the Atmoshpere and Ocean, University of Washington, Seattle).

Dalton, M. M., Mote, P. W., & Snover, A. K. (Eds.). (2013). *Climate Change in the Northwest: Implications for Our Landscapes, Waters and Communities*. Washington, D.C.: Island Press.

Dawson, J., Scott, D., & McBoyle, G. (2009). Climate change analogue analysis of ski tourism in the northeastern USA. *Climate Research*, *39*, 1–9. https://doi.org/10.3354/cr00793

ECMWF (2015). ecFlow User's Guide. Reading, UK: European Centre for Medium Range Weather Forecasts. Retrieved from: https://software.ecmwf.int/wiki/display/ECFLOW/Documentation

Elsasser, H., & Bürki, R. (2002). Climate change as a threat to tourism in the Alps. *Climate Research*, *20*, 253–257. https://doi.org/10.3354/cr020253

Elsner, M. M., Cuo, L., Voisin, N., Deems, J. S., Hamlet, A. F., Vano, J. A., … Lettenmaier, D. P. (2010). Implications of 21st century climate change for the hydrology of Washington State. *Climatic Change*, *102*(1-2), 225–260. https://doi.org/10.1007/s10584-010-9855-0

Gao. H., Tang, Q., Shi, X., Zhu, C, Bohn, T. J., Su, F. Sheffield, J., Pan, M., Lettenmaier, D. P., & Wood, E. F. (In review). Water Budget Record from Variable Infiltration Capacity (VIC) Model. *Algorithm Theoretical Basis Document for Terrestrial Water Cycle Data Records.*

Gergel, D. R., B. Nijssen, J. T. Abatzoglou, D. P. Lettenmaier, M. R. Stumbaugh, 2016: Effects of climate change on snowpack and fire potential in the western United States. *Climatic Change*. In revision.

Hamlet, A. F., Carrasco, P., Deems, J., Elsner, M. M., Kamstra, T., Lee, C., … Whitely Binder, L. (2010). *Final Project Report for the Columbia Basin Climate Change Scenarios Project*. Retrieved from http://warm.atmos.washington.edu/2860/report/

Hamlet, A. F., & Lettenmaier, D. P. (1999). Effects of Climate Change on Hydrology and Water Resources in the Columbia River Basin. *Journal of the American Water Resources Association*, *35*(6), 1597–1623. https://doi.org/10.1111/j.1752-1688.1999.tb04240.x

Hamman, J., Nijssen, B., Lettenmaier, D. P., Naz, B., Fyke, J. (2014). A Macroscale Glacier Model to Evaluate Climate Change Impacts in the Columbia River Basin. Presentation given at the 5th Annual Pacific Northwest Climate Conference, University of Washington, Seattle, Washington. Retrieved from: www.pnwclimateconference.org/2014presentations/Hamman.pdf

Hamlet, A. F., Mote, P. W., Snover, A. K., Lettenmaier, D. P. (Unpublished). Effects of Climate Change on the Pacific Northwest Ski Industry. Poster. JISAO CSES Climate Impacts Group Department of Civil and Environmental Engineering University of Washington.

Hamman, J., Nijssen, B., Bohn, T., Franssen, W., Mao, Y., homefc, … apcraig. (2016). VIC: VIC.5.0.0. https://doi.org/10.5281/zenodo.61423

Hennessy KJ, Whetton PH, Bathols J, Hutchinson M, Sharples J (2003). The impact of climate change on snow conditions in Australia. Consultancy report for the Victorian Dept of Sustainability and Environment, NSW National Parks and Wildlife Service, Australian Green-house Office and the Australian Ski Areas Association. CSIRO Atmospheric Research, Aspendale. Available at: www.cmar.csiro.au/e-print/open/hennes sy_2003a.pdf

IPCC (2014). Climate Change 2014: Synthesis Report. Contribution of Working Groups I, II and III to the Fifth Assessment Report of the Intergovernmental Panel on Climate Change [Core Writing Team, R. K. Pachauri and L. A. Meyers (eds.)]. IPCC, Genevea, Switzerland.

IPCC (1995). IPCC Second Assessment, Climate Change 1995: A Report of the Intergovernmental Panel on Climate Change. Retrieved from: https://www.ipcc.ch/pdf/climate-changes-1995/ipcc-2nd-assessment/2nd-assessment-en.pdf

Kirtman, B. P., Min, D., Infanti, J. M., Kinter, J. L., Paolino, D. A., Zhang, Q., … Wood, E. F. (2014). The North American Multimodel Ensemble: Phase-1 Seasonal-to-Interannual Prediction; Phase-2 toward Developing Intraseasonal Prediction. *Bulletin of the American Meteorological Society*, *95*(4), 585–601. https://doi.org/10.1175/BAMS-D-12-00050.1

Koenig, U., & Abegg, B. (1997). Impacts of Climate Change on Winter Tourism in the Swiss Alps. *Journal of Sustainable Tourism*, *5*(1), 46–58. https://doi.org/10.1080/09669589708667275

Liang, X., Lettenmaier, D. P., Wood, E. F., & Burges, S. J. (1994). A simple hydrologically based model of land surface water and energy fluxes for general circulation models. *Journal of Geophysical Research*, *99*(D7), 14, 415–14, 428. https://doi.org/10.1029/94JD00483

Livneh, B., E. Rosenberg, C. Lin, B. Nijssen, V. Mishra, K. Andreadis, E. Maurer, and Lettenmaier, D. P. (2013). A Long-Term Hydrologically Based Dataset of Land Surface Fluxes and States for the Conterminous United States: Update and Extensions. *J. Climate,* 26, 9384–9392, doi: 10.1175/JCLI-D-12-00508.1.

Leavesley, G.H., Lichty, R.W., Troutman, B.M., and Saindon, L.G. (1983). Precipitation-runoff modeling system—User's manual: U.S. Geol. Surv. Water Resour. Invest. Rep. 83-4238.

Markstrom, S. L., Regan, R. S., Hay, L. E., Viger, R. J., Webb, R. M. T., Payn, R. A., & LaFontaine, J. H. (2015). *PRMS-IV, the Precipitation-Runoff Modeling System, Version 4:*

U. S. Geological Survey Techniques and Methods, book 6, chap B7. https://dx.doi.org/10.3133/tm6B7

Meehl, G. A., Covey, C., Taylor, K. E., Delworth, T., Stouffer, R. J., Latif, M., … Mitchell, J. F. B. (2007). THE WCRP CMIP3 Multimodel Dataset: A New Era in Climate Change Research. *Bulletin of the American Meteorological Society*, *88*(9), 1383–1394. https://doi.org/10.1175/BAMS-88-9-1383

Mote, P. W. (2003a). Trends in Temperature and Precipitation in the Pacific Northwest During the Twentieth Century. *Northwest Science*, *77*(4), 271–282.

Mote, P. W. (2003b). Trends in snow water equivalent in the Pacific Northwest and their climatic causes. *Geophysical Research Letters*, *30*(12). https://doi.org/10.1029/2003GL017258

Mote, P. W., & Salathé, E. P. (2010). Future climate in the Pacific Northwest. *Climatic Change*, *102*(1-2), 29–50. https://doi.org/10.1007/s10584-010-9848-z

Mote, P. W., D. E. Rupp, S. Li, D. J. Sharp, F. Otto, P. F. Uhe, M. Xiao, D. P. Lettenmaier, H. Cullen, and M. R. Allen (2016). Perspectives on the causes of exceptionally low 2015 snowpack in the western United States, Geophys. Res. Lett., 43, 10,980–10,988, doi:10.1002/2016GL069965.

Nolin, A. and C. Daly, 2006: Mapping "At Risk" Snow in the Pacific Northwest. *J. Hydrometeor.*, **7**, 1164–1171, doi: 10.1175/JHM543.1.

Northrop, P. J. and Chandler, R. E. (2014). Quantifying Sources of Uncertainty in Projections of Future Climate. J. Climate, 27, 8793–8808, doi: 10.1175/JCLI-D-14-00265.1.

Pan, M., & Wood, E. F. (2013). Inverse streamflow routing. *Hydrology and Earth System Sciences*, *17*(11), 4577–4588. https://doi.org/10.5194/hess-17-4577-2013

Payne, J. T., Wood, A. W., Hamlet, A. F., Palmer, R. N., & Lettenmaier, D. P. (2004). Mitigating the Effects of Climate Change on the Water Resources of the Columbia River Basin. *Climatic Change*, *62*(1-3), 233–256. https://doi.org/10.1023/B:CLIM.0000013694.18154.d6

Prata, A.J., 1996. A new long-wave formula for estimating downward clearsky radiation at the surface. Q. J. R. Meteor. Soc. 122 (533), 1127–1151, http://dx.doi.org/10.1002/qj.49712253306.

Rahman, M., & Lu, M. (2015). Model Spin-Up Behavior for Wet and Dry Basins: A Case Study Using the Xinanjiang Model. *Water*, *7*(8), 4256–4273. https://doi.org/10.3390/w7084256

Rupp, D. E., J. T. Abatzoglou, K. C. Hegewisch, and P. W. Mote (2013), Evaluation of CMIP5 20th century climate simulations for the Pacific Northwest USA, J. Geophys. Res. Atmos., 118, 10,884–10,906, doi:10.1002/jgrd.50843.

Scott, D., Dawson, J., & Jones, B. (2008). Climate change vulnerability of the US Northeast winter recreation– tourism sector. *Mitigation and Adaptation Strategies for Global Change*, *13*(5-6), 577–596. https://doi.org/10.1007/s11027-007-9136-z

Scott, D., McBoyle, G., & Minogue, A. (2007). Climate change and Quebec's ski industry. *Global Environmental Change*, *17*(2), 181–190. https://doi.org/10.1016/j.gloenvcha.2006.05.004

Scott, D., Mcboyle, Mills, B., & Minogue. (2006). Climate change and the sustainability of ski-based tourism in eastern North America. *Journal of Sustainable Tourism*, *14*(4), 376–298.

Shukla, S., Steinemann, A. C., & Lettenmaier, D. P. (2011). Drought Monitoring for Washington State: Indicators and Applications. *Journal of Hydrometeorology*, *12*(1), 66–83. https://doi.org/10.1175/2010JHM1307.1

Steele, M. O., Chang, Heejun, Reusser, D. A., Brown, C. A., & Jung, I. -W. (2012). Potential Climate-Induced Runoff Changes and Associated Uncertainty in Four Pacific Northwest Estuaries: U. S. Geological Survey Open-File Report 2012-1274.

Stewart, I. T., Cayan, D. R., & Dettinger, M. D. (2005). Changes toward Earlier Streamflow Timing across Western North America. *Journal of Climate*, *18*(8), 1136–1155. https://doi.org/10.1175/JCLI3321.1

Sumioka, S.S., Kresch, D.L. & Kasnick, K.D. (1998). Magnitude and Frequency of Floods in Washington. U. S. Geological Survey, Water-Resources Investigations Report 97-4277. Retrieved from http://pubs.usgs.gov/wri/1997/4277/report.pdf

Taylor, K. E., Stouffer, R. J., & Meehl, G. A. (2012). An Overview of CMIP5 and the Experiment Design. *Bulletin of the American Meteorological Society*, *93*(4), 485–498. https://doi.org/10.1175/BAMS-D-11-00094.1

Vano, J. A., Scott, M., Voisin, N., Stöckle, C. O., Hamlet, A. F., Mickelson, K. E. B., ... Lettenmaier, D. P. (2010). Climate change impacts on water management and irrigated

agriculture in the Yakima River basin, Washington, USA. Climatic Change, 102(1–2). doi:10.1007/s10584-010-9856-z

Wood, A. W. (2002). Long-range experimental hydrologic forecasting for the eastern United States. *Journal of Geophysical Research, 107*(D20). https://doi.org/10.1029/2001JD000659

Wood, A. W. (2008). The University of Washington Surface Water Monitor: an experimental platform for national hydrologic assessment and prediction. Presented at the AMS 22nd Conference on Hydrology.

Wood, A. W., & Lettenmaier, D. P. (2006). A Test Bed for New Seasonal Hydrologic Forecasting Approaches in the Western United States. *Bulletin of the American Meteorological Society, 87*(12), 1699–1712. https://doi.org/10.1175/BAMS-87-12-1699

Xiao, M., B. Nijssen, and D. Lettenmaier, 2016: Drought in the Pacific Northwest, 1920–2013. *J. Hydrometeor.*, **17**, 2391–2404, doi: 10.1175/JHM-D-15-0142.1.

Yang, Z.-L., Dickinson, R. E., Henderson-Sellers, A., & Pitman, A. J. (1995). Preliminary study of spin-up processes in land surface models with the first stage data of Project for Intercomparison of Land Surface Parameterization Schemes Phase 1(a). *Journal of Geophysical Research, 100*(D8), 16553. https://doi.org/10.1029/95JD01076

Appendix 1: Projected changes in temperature and precipitation, supplemental figures

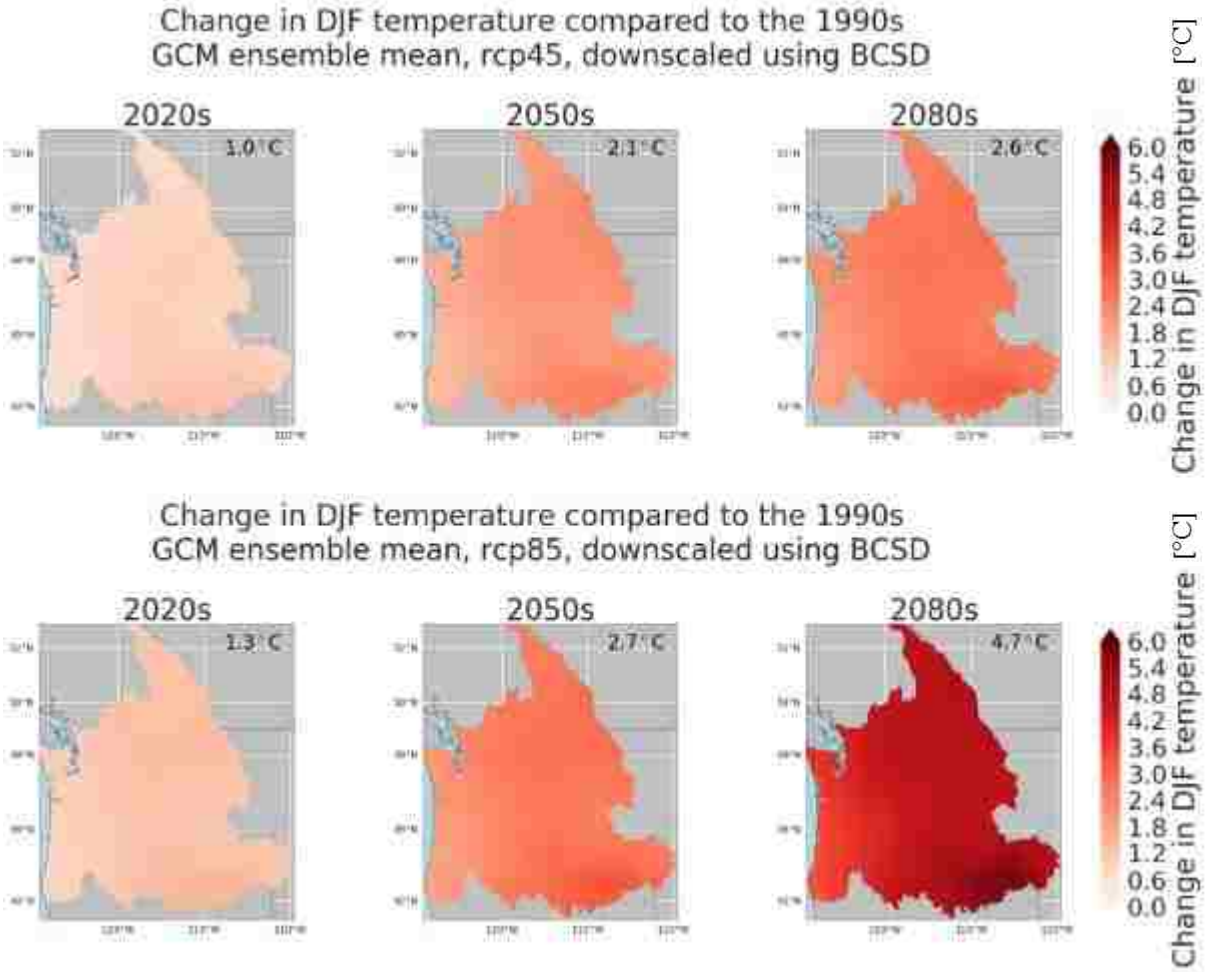

Figure A.1.1: Winter temperature change projections for the Columbia River Basin and coastal drainages for RCP 4.5 and RCP 8.5 (GCM ensemble mean, downscaled using BCSD).

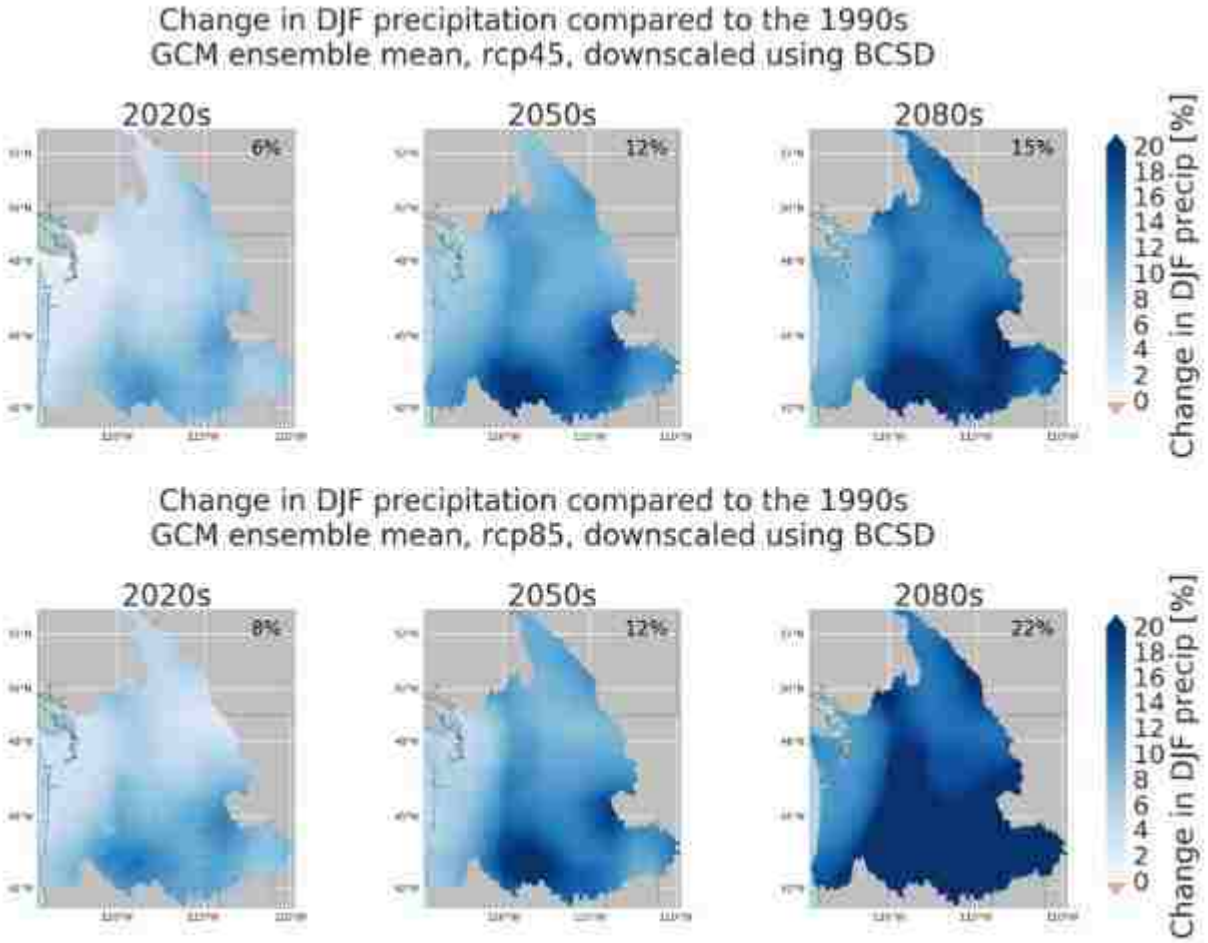

Figure A.1.2: Winter precipitation change projections for the Columbia River Basin and coastal drainages for RCP 4.5 and RCP 8.5 (GCM ensemble mean, downscaled using BCSD).

Appendix 2: Projected changes in snowpack, supplemental figures

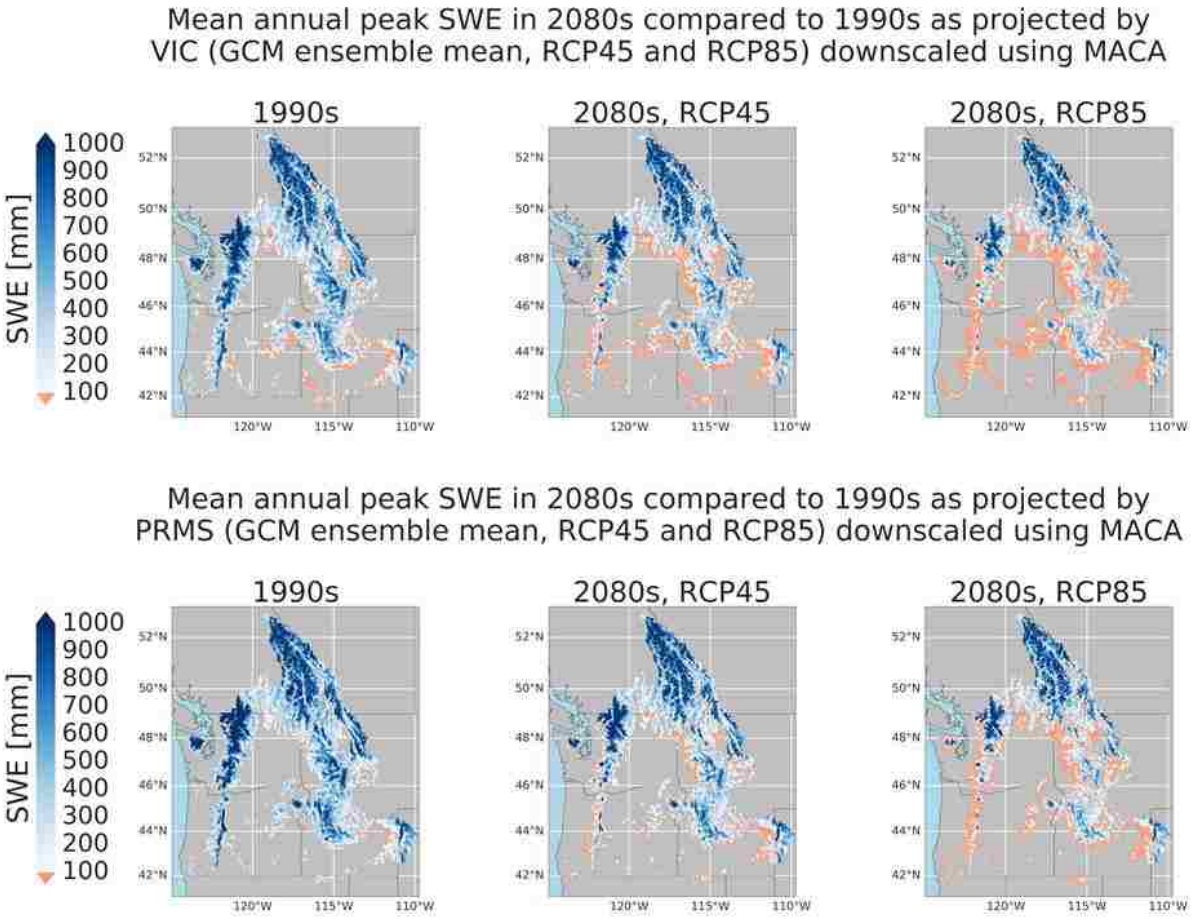

Figure A.2.1: Mean annual peak SWE in 2080s compared to 1990s as projected by VIC and PRMS (GCM ensemble mean) for both RCP 4.5 and 8.5 (downscaled by MACA downscaling method). Note that grid cells with mean April 1 SWE < 10mm in the historic period are masked out.

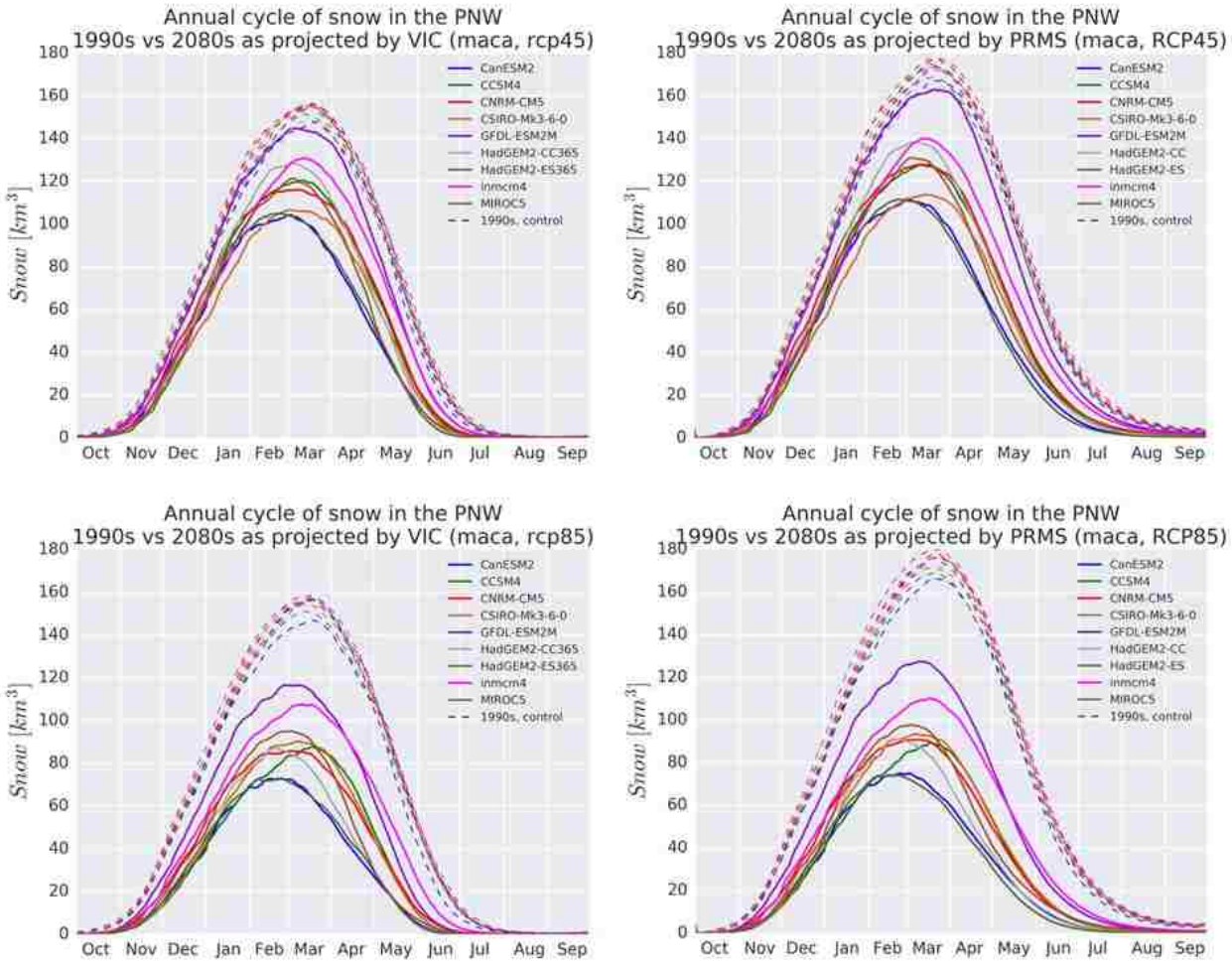

Figure A.2.2: The annual cycle of volumetric SWE in the PNW. The 1990s are compared with the 2080s as projected by VIC and PRMS and 10 GCMs (downscaled using MACA).